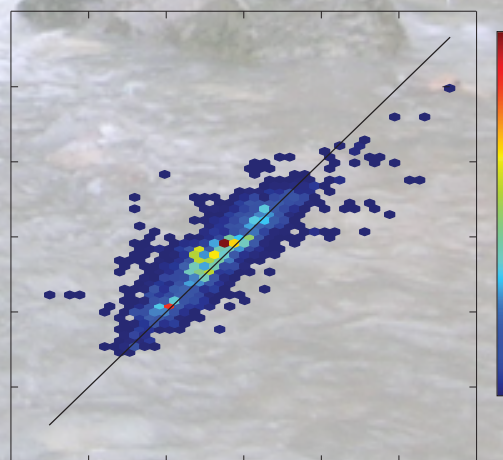
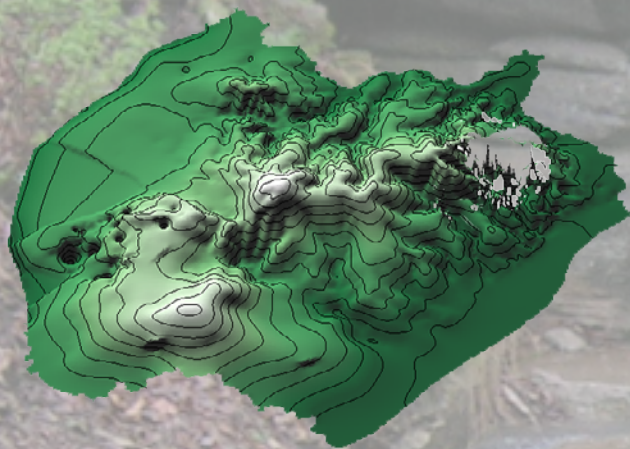


Water Availability and Use Science Program

The Ozark Plateaus Regional Aquifer Study—Documentation of a Groundwater-Flow Model Constructed to Assess Water Availability in the Ozark Plateaus



Scientific Investigations Report 2018–5035

U.S. Department of the Interior
U.S. Geological Survey

The Ozark Plateaus Regional Aquifer Study—Documentation of a Groundwater-Flow Model Constructed to Assess Water Availability in the Ozark Plateaus

By Brian R. Clark, Joseph M. Richards, and Katherine J. Knierim

Water Availability and Use Science Program

Scientific Investigations Report 2018–5035

**U.S. Department of the Interior
U.S. Geological Survey**

U.S. Department of the Interior

RYAN K. ZINKE, Secretary

U.S. Geological Survey

William H. Werkheiser, Deputy Director
exercising the authority of the Director

U.S. Geological Survey, Reston, Virginia: 2018

For more information on the USGS—the Federal source for science about the Earth, its natural and living resources, natural hazards, and the environment—visit <https://www.usgs.gov> or call 1–888–ASK–USGS.

For an overview of USGS information products, including maps, imagery, and publications, visit <https://store.usgs.gov>.

Any use of trade, firm, or product names is for descriptive purposes only and does not imply endorsement by the U.S. Government.

Although this information product, for the most part, is in the public domain, it also may contain copyrighted materials as noted in the text. Permission to reproduce copyrighted items must be secured from the copyright owner.

Suggested citation:

Clark, B.R., Richards, J.M., and Knierim, K.J., 2018, The Ozark Plateaus Regional Aquifer Study—Documentation of a groundwater-flow model constructed to assess water availability in the Ozark Plateaus: U.S. Geological Survey Report 2018–5035, 33 p., <https://doi.org/10.3133/sir20185035>.

ISSN 2328-0328 (online)

Contents

Abstract.....	1
Introduction.....	1
Purpose and Scope	2
Study Area	2
Hydrogeologic Units	2
Groundwater-Flow Model Construction	2
Spatial Discretization and Layering	6
Temporal Discretization	6
Areal Recharge	6
Groundwater Pumpage.....	9
Hydrologic Boundaries	10
Streams.....	10
Specified-Head and No-Flow Boundaries.....	10
Saline-Freshwater Interface.....	12
Faults	12
Hydraulic Properties.....	12
Hydraulic Conductivity.....	12
Storage	13
Model History Matching	13
Weighted Hydraulic-Head Observations	13
Stream Leakage as Observations	14
Model Evaluation	14
Optimal Parameter Estimates	14
Model Fit and Model Error.....	14
Hydraulic-Head Observations and Errors.....	14
Streamflow Observations and Errors	22
Simulated and Observed Hydrographs	22
Simulated and Observed Potentiometric Surfaces.....	23
Sensitivity and Identifiability.....	23
Groundwater-Flow Budget.....	25
Limitation of Analysis	25
Summary.....	30
References Cited.....	31

Figures

1. Map showing surficial geology and structural features of the Ozark Plateaus aquifer system.....3
2. Stratigraphic column showing generalized correlation of Paleozoic units and regional hydrogeologic units of the Ozark Plateaus aquifer system with corresponding model layer number
3. Map showing pilot-point distribution with final calibrated values of average, model adjusted recharge from 2000 to 2013.....7

4. Map showing head-dependent flux, specified head, and horizontal flow boundaries implemented in the Ozark model.....	11
5. Maps showing horizontal and vertical hydraulic conductivity of model layers that utilize pilot points	18
6. Histogram of all unweighted hydraulic-head residuals	22
7. Graph of unweighted simulated hydraulic-head values plotted against observed.	23
8. Map showing spatial distribution of hydraulic-head residuals for the lower Ozark aquifer excluding observations categorized as “poor.”	24
9. Graph of simulated stream leakage plotted against observed stream leakage	25
10. Hydrographs showing simulated and observed water levels in selected wells	26
11. Map showing the potentiometric surface and simulated water levels for the Ozark aquifer, winter of 2014–15	27
12. Bar graph showing parameter group sensitivities.....	28
13. Bar graph showing parameter identifiability of the top 30 pilot-point parameters in the model	29
14. Graphs showing groundwater-flow budget of large water-budget components and small water-budget components.....	30

Tables

1. Stress period discretization used in the Ozark model	8
2. Final parameter estimates.....	15
3. Summary of hydraulic-head residual statistics for model calibration	19

Conversion Factors

U.S. customary units to International System of Units

Multiply	By	To obtain
Length		
foot (ft)	0.3048	meter (m)
mile (mi)	1.609	kilometer (km)
Area		
square mile (mi ²)	259.0	hectare (ha)
square mile (mi ²)	2.590	square kilometer (km ²)
Flow rate		
cubic foot per second (ft ³ /s)	0.02832	cubic meter per second (m ³ /s)
million gallons per day (Mgal/d)	0.04381	cubic meter per second (m ³ /s)
inch per year (in/yr)	25.4	millimeter per year (mm/yr)
Hydraulic conductivity		
foot per day (ft/d)	0.3048	meter per day (m/d)
Transmissivity*		
foot squared per day (ft ² /d)	0.09290	meter squared per day (m ² /d)

Datum

Horizontal coordinate information is referenced to the North American Datum of 1983 (NAD 83).

Vertical coordinate information is referenced to the North American Vertical Datum of 1988 (NAVD 88).

Altitude, as used in this report, refers to distance above the vertical datum.

Abbreviations

CHD	Constant-Head Boundary
DEM	Digital elevation model
EWB	Empirical Water Balance
GHB	General-Head Boundary
HFB	Horizontal-Flow Boundary
MERAS	Mississippi embayment regional aquifer system
NHDPlus	National Hydrography Dataset
PEST	Parameter estimation software
RCH	Recharge Package
RIV	River Package
RMSE	Root mean square error
RVOB	River Observation Package
SFR2	Streamflow-Routing Package
SWB	Soil-Water Balance
USGS	U.S. Geological Survey
WEL	Well Package
7Q2	7-day, 2-year streamflow

The Ozark Plateaus Regional Aquifer Study— Documentation of a Groundwater-Flow Model Constructed to Assess Water Availability in the Ozark Plateaus

By Brian R. Clark, Joseph M. Richards, and Katherine J. Knierim

Abstract

Recent short-term drought conditions have emphasized the need to better understand the delicate balance between abundance, sustainability, and scarcity of groundwater in the Ozark Plateaus aquifer system. In 2014, the U.S. Geological Survey began construction of a groundwater-flow model as a tool for the assessment of groundwater availability in the Ozark Plateaus aquifer system. The model was developed to benefit concurrent and future investigations involving groundwater-pumping scenarios, optimization, particle transport, and groundwater-monitoring network analysis.

The groundwater model simulates 116 years (1900–2015) of hydrologic conditions and the response of the groundwater system to changes in stress including changes in recharge and groundwater pumping for water supply. Semiseasonal stress periods were simulated from the later part of 1991 to 2015 and represent higher demand and lower recharge in the spring and summer months and lower demand and higher recharge in the fall and winter months. Groundwater pumping increases throughout the simulation period with a maximum rate of about 600 million gallons per day (Mgal/d).

The process of matching historical hydrologic data for the Ozark Plateaus aquifer system model was accomplished by a combination of manual changes to parameter values and automated calibration methods. Observation data used in the development and evaluation of the model included 19,045 hydraulic-head observations from 6,683 wells within the model area. Observation data also included stream leakage estimates summed to calculate a net gain or net loss value for approximately 81 named streams.

The majority (mean of over 95 percent) of the recharge component is discharged through streams simulated in the model. The total simulated discharge to streams fluctuates seasonally between 7,500 and 17,500 Mgal/d with a mean outflow of 11,500 Mgal/d. Much of the remaining balance between modeled recharge inflows and stream outflows is made up by water moving into or out of storage in the aquifer system resulting in changes in modeled groundwater levels.

The goal of the model was to develop a model capable of suitable accuracy at regional scales. The intent was not to reproduce individual local-scale details, which are typically not possible given the uniform cell size of 1 square mile. Although the model may not represent each local-scale detail, the model can be applied for a better understanding of the regional flow system and to evaluate responses to changes in climate and groundwater pumping.

Introduction

Fresh groundwater in the Ozark Plateaus aquifer system (hereafter referred to as the Ozark system) is a source for municipal, industrial, agricultural, and domestic water supply needs across much of southern Missouri, northern Arkansas, and smaller areas of southeastern Kansas and northeastern Oklahoma. Groundwater generally occurs in abundance throughout the Ozark system, however, recent (2012) short-term drought conditions have emphasized the delicate balance between groundwater use and water abundance and scarcity. The relatively large regional extent and socioeconomic importance of the Ozark system made the area the focus of a groundwater availability study supported by the Water Availability and Use Science Program of the U.S. Geological Survey (USGS, 2016). The fractured and karst character of the Ozark system, coupled with relatively slow recharge rates, results in low hydraulic storage that restricts the capacity of the aquifer to sustain water supplies through drought periods longer than a few years. The current study conducted by the USGS developed a groundwater-flow model as the primary tool to assess groundwater availability in the Ozark system. The groundwater-flow model can be applied to simulate and evaluate regional scenarios of changing groundwater pumping and changing climate. Additionally, the model may be used to determine the influence of an increase in the number and types of observations that could reduce uncertainty in parameter values and thus decrease the uncertainty associated with future predictions.

of groundwater-level altitudes or flow. Although model scenarios and data value analysis are beyond the scope of the current report, they are part of ongoing work to quantify the groundwater availability of the Ozark system. All archive data for this model are available from a USGS data release (Duncan and Clark, 2018).

Purpose and Scope

This report documents the development of a numerical model representing regional groundwater flow in the Ozark system and the process of matching historical hydrologic data (history-matching), which serves to ensure the numerical model represents measured or estimated conditions. The model is intended to support the estimation of available groundwater in the Ozark system. Additionally, the model provides a quantitative tool to benefit current and future investigations involving groundwater-pumping scenarios, optimization, particle transport, and groundwater-monitoring network analysis. The scope of the study spans a temporal range from 1900 to 2015, a horizontal extent of 68,000 square miles (mi²) in Arkansas, Kansas, Missouri, and Oklahoma, and a vertical extent from land surface to Precambrian basement rock (several thousand feet below land surface in some areas).

Study Area

The Ozark system study area, referred to as the model area in this report (fig. 1), is bounded by the Missouri River to the north, the Mississippi River to the east, the Mississippi embayment to the southeast, the Arkansas River to the south, and the broad and gentle regional topographic low extending from northeastern Oklahoma to the Missouri River to the west. The climate of the Ozark Plateaus is temperate because of the mid-latitude, interior-continent location (Adamski and others, 1995). Mean annual precipitation for the climatological period of 1900–2014 varied spatially from approximately 43.2 inches per year (in/yr) across the northern part to 49.5 in/yr across the southern part, with an overall mean of 43.9 in/yr (Hays and others, 2016). Precipitation varies seasonally, with a generally drier winter period (January, February, March) and wetter spring (April, May, June) (Hays and others, 2016). The estimated mean annual evapotranspiration ranges from 30 to 35 in/yr (Adamski and others, 1995) and also varies seasonally with the highest rates typically in the summer (July, August, September) when temperatures are highest (Brye and others, 2004; Hays and others, 2016).

Prior to European settlement, land cover in the Ozark Plateaus was primarily forest on the hilly regions and prairie in the western part of the study area (Adamski and others, 1995). Recent land cover or land use consists primarily of forest (48 percent) and agriculture (40 percent) with local urban development (7 percent) (Hays and others, 2016). Groundwater pumping is related to land use with dispersed domestic, livestock, and agricultural use in forested, hay,

pasture, and cultivated crop area and public supply and industrial use concentrated around urban centers (Hays and others, 2016; Knierim and others, 2017).

Hydrogeologic Units

The Ozark system is composed of relatively flat-lying, interbedded carbonate and clastic lithologies, with sandstone and karstified limestone units serving as primary aquifers and shale or dense dolomite serving as confining units (Jorgensen and others, 1993; Imes and Emmett, 1994; Hays and others, 2016). Hydrogeologic units include the Western Interior Plains confining system, Springfield Plateau aquifer, Ozark confining unit, Ozark aquifer, St. Francois confining unit, and the St. Francois aquifer (fig. 2). For the productive hydrogeologic units, aquifers are generally unconfined where units are exposed at surface and confined where overlain by regional confining units. As noted in Westerman and others (2016b), the Ozark aquifer is divided into three sections (the upper, middle, and lower Ozark aquifer) based on differences in hydrologic characteristics. The middle Ozark aquifer includes dolomite with relatively low permeability, such that the unit regionally acts as a confining unit. The Ozark aquifer (primarily the lower aquifer) is the most productive, thus the most widely used aquifer for groundwater supply of any hydrogeologic unit in the Ozark system (Hays and others, 2016; Westerman and others, 2016b). Median thickness of units ranges from over 1,800 feet (ft) (Ozark aquifer) to less than 50 ft (Ozark confining unit) (Westerman and others, 2016a, 2016b). In some areas, units pinch out or are absent (Hays and others, 2016). The base of the system is the basement unit, which includes Precambrian-age igneous and metamorphic rocks (fig. 2).

Groundwater-Flow Model Construction

The Ozark system was simulated by using the USGS MODFLOW-NWT (Niswonger and others, 2011) groundwater-flow model code to approximate the solution of equations governing three-dimensional groundwater flow. The groundwater-flow system is represented by a set of three-dimensional cells within which the hydraulic properties are uniform. The finite-difference equations describing groundwater flow through each cell can be solved for either steady-state or transient conditions to simulate water-level changes within the flow system resulting from pumping stress over discrete periods of time. The model simulates 116 years (1900–2015) of system response to stress by using 79 stress periods.

Hydraulic conductivity, recharge, streambed conductivity, vertical conductivity, and storage values vary spatially through the use of pilot points (Doherty, 2003). Pilot points are incorporated by specifying a point at a location with a value (or multiplier) of a hydraulic property, which can change throughout the history-matching process, whereby

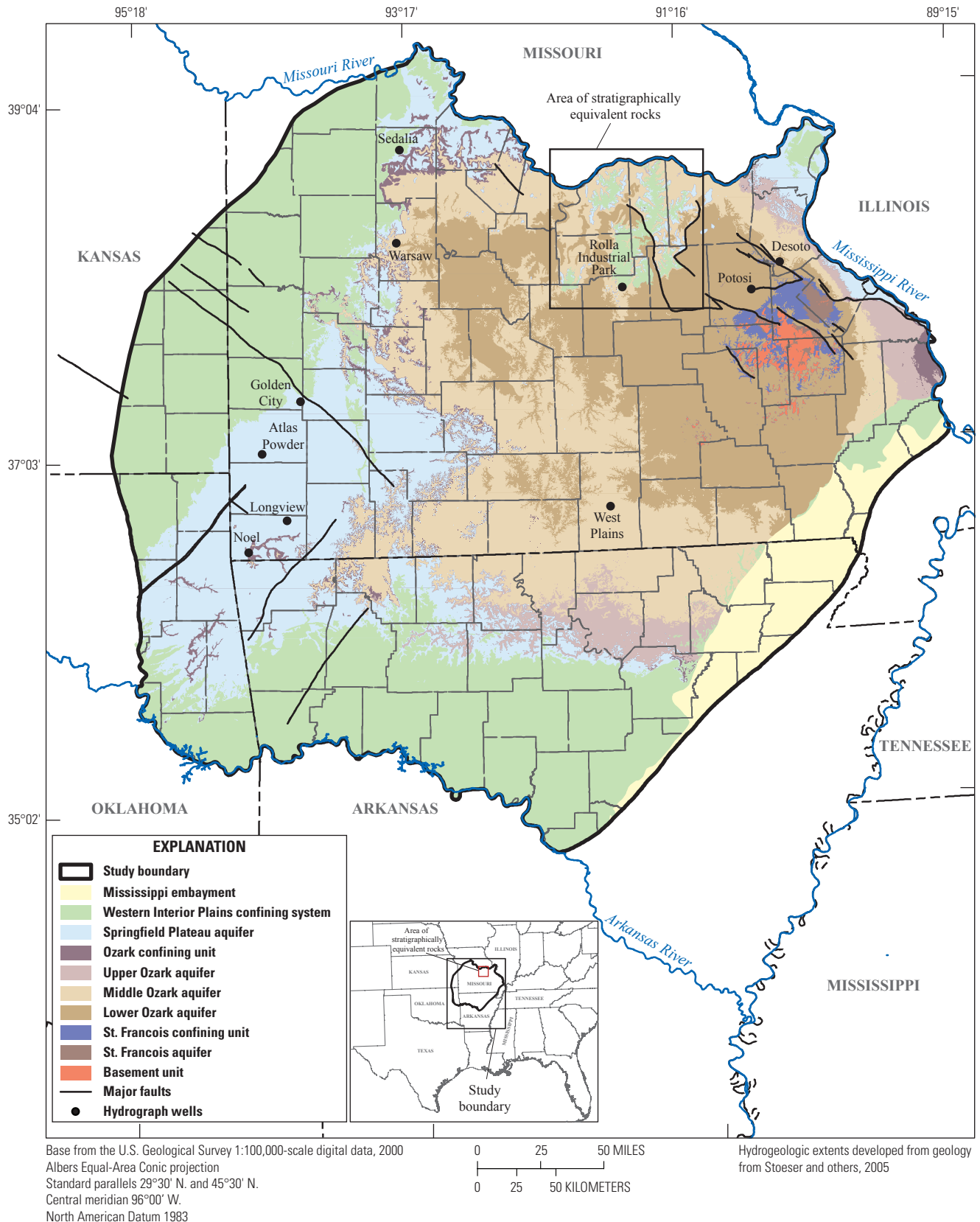


Figure 1. Surficial geology and structural features of the Ozark Plateaus aquifer system.

4 The Ozark Plateaus Regional Aquifer Study—Documentation of a Groundwater-Flow Model

Era	System	Southeastern Missouri	Southwestern Missouri	Southeastern Kansas	Northeastern Oklahoma	Northern Arkansas	Aquifers and confining units described in the report		Model layer
							Hydrogeologic unit	Hydrogeologic system	
Paleozoic	Pennsylvanian	Pleasanton Formation ¹ Marmaton Group ¹ Cherokee Shale ¹	Kansas City Group Pleasanton Formation Marmaton Group Cherokee Shale	Kansas City Group Pleasanton Group Marmaton Group Cherokee Group	Marmaton Group Cabiniss Group Krebs Group Atoka Formation Boyd Shale Hale Formation	McAlester Formation Hartshorne Sandstone Atoka Formation Boyd Shale Hale Formation	Western Interior Plains confining system ²		Layer 1
		Vienna Limestone ^{1,4} Tar Springs Sandstone ^{1,4} Glen Dean Limestone ^{1,4} Hardinsburg Sandstone ^{1,4} Golconda Formation ^{1,4} Cypress Formation ^{1,4} Paint Creek Formation ^{1,4} Yankeetown Sandstone ^{1,4} Renault Formation ^{1,4} Aux Vases Sandstone ¹	Fayetteville Shale Batesville Sandstone Hindsville Limestone Carterville Formation	Fayetteville Shale Batesville Sandstone Hindsville Limestone	Pitkin Limestone	Pitkin Limestone			
		St. Genevieve Limestone ³		Moorefield Formation	Moorefield Formation	Moorefield Formation			
		St. Louis Limestone ³ Salem Limestone ³ Warsaw Limestone ³ Keokuk Limestone ³ Burlington Limestone ³	St. Louis Limestone Salem Limestone Warsaw Limestone Keokuk Limestone ⁴ Burlington Limestone Elsey Formation Reeds Spring Formation Pierson Formation ⁴	St. Louis Limestone Salem Limestone Warsaw Limestone Keokuk Limestone ⁴ Burlington Limestone	Boone Formation Reeds Spring Member St. Joe Limestone Member	Boone Formation Reeds Spring Member St. Joe Limestone Member			
		Fern Glen Limestone ³		Fern Glen Limestone	Boone Formation Reeds Spring Member St. Joe Limestone Member	Boone Formation Reeds Spring Member St. Joe Limestone Member			
	Mississippian	Chouteau Limestone Hannibal Shale Bachelor Formation ⁴ Bushberg Sandstone Glen Park Limestone Chattanooga Shale	Northview Shale Sedalia Limestone Compton Limestone	Chouteau Limestone	Northview Equivalent ⁶ Compton Equivalent ⁶	Ozark confining unit	Ozark Plateaus aquifer system ⁵		Layer 2
				Woodford Chert Chattanooga Shale	Chattanooga Shale				
				Chattanooga Shale	Chattanooga Shale				
				Chattanooga Shale	Chattanooga Shale				
				Chattanooga Shale	Chattanooga Shale				
	Devonian	St. Laurent Limestone Grand Tower Limestone Clear Creek Chert ⁴ Little Saline Limestone Railev Limestone	Callaway Formation Fortune Formation ⁴	Chattanooga Shale	Salisaw Formation Frisco Limestone	Upper Ozark aquifer	Ozark Plateaus aquifer system ⁵		Layer 3
									Layer 4

Figure 2. Generalized correlation of Paleozoic units and regional hydrogeologic units of the Ozark Plateaus aquifer system with corresponding model layer number. Modified from Hays and others (2016).

Paleozoic	Silurian	Bainbridge Limestone	Kimmiswick Limestone			St. Clair Limestone	Lafferty Limestone St. Clair Limestone Brassfield Limestone	Ozark aquifer	Ozark Plateaus aquifer system ⁵	
		Sexton Creek Limestone ⁴								
	Ordovician	Girardeau Limestone	Kimmiswick Limestone			Sylvan Shale Fernvale Limestone Viola Limestone Fite Limestone Tyner Formation Burgin Sandstone Smithville Equivalent Powell Dolomite	Cason Shale Fernvale Limestone Kimmiswick Limestone			
		Orchard Creek Shale								
		Thebes Sandstone								
		Maquoketa Shale								
		Cape Limestone ⁴								
		Decorah Formation								
		Plattin Limestone								
		Rock Levee Formation ⁴								
Cambrian		Joachim Dolomite	Kimmiswick Limestone			Cotter Dolomite Jefferson City Dolomite Roubidoux Formation Gasconade Dolomite Van Buren Formation ⁴ Gunter Sandstone Member ⁴ Eminence Dolomite Potosi Dolomite ⁶ Doe Run Dolomite Derby Dolomite Davis Formation Bonnetterre Dolomite ⁶ Reagan Sandstone ⁴ Lamotte Sandstone	Plattin Limestone			
		Dutchtown Formation ⁴								
		St. Peter Sandstone								
		Everton Formation								
		Smithville Formation								
		Powell Dolomite								
		Cotter Dolomite								
		Jefferson City Dolomite								
		Gasconade Dolomite								
		Van Buren Formation ⁴								
		Member ⁴	Kimmiswick Limestone			Cotter Dolomite Jefferson City Dolomite Roubidoux Formation Gasconade Dolomite Van Buren Formation ⁴ Gunter Sandstone Member ⁴ Eminence Dolomite Potosi Dolomite ⁶ Doe Run Dolomite Derby Dolomite Davis Formation Bonnetterre Dolomite ⁶ Reagan Sandstone Lamotte Sandstone	Joachim Dolomite			
		Gunter Sandstone								
		Member ⁴								
		Eminence Dolomite								
		Potosi Dolomite								
		Doe Run Dolomite								
		Derby Dolomite								
		Davis Formation								
		Bonnetterre Formation ⁶								
		Reagan Sandstone ⁴								
Lamotte Sandstone										
		Gasconade Dolomite	Kimmiswick Limestone			Cotter Dolomite Jefferson City Dolomite Roubidoux Formation Gasconade Dolomite Van Buren Formation ⁴ Gunter Sandstone Member ⁴ Eminence Dolomite Potosi Dolomite ⁶ Doe Run Dolomite Derby Dolomite Davis Formation Bonnetterre Dolomite ⁶ Reagan Sandstone Lamotte Sandstone	St. Peter Sandstone Everton Formation Smithville Formation Powell Dolomite			
		Van Buren Formation ⁴								
		Gunter Sandstone								
		Member ⁴								
		Eminence Dolomite								
		Potosi Dolomite								
		Doe Run Dolomite								
		Derby Dolomite								
		Davis Formation								
		Bonnetterre Formation ⁶								
Reagan Sandstone ⁴										
Lamotte Sandstone										
		Gasconade Dolomite	Kimmiswick Limestone			Cotter Dolomite Jefferson City Dolomite Roubidoux Formation Gasconade Dolomite Van Buren Formation ⁴ Gunter Sandstone Member ⁴ Eminence Dolomite Potosi Dolomite ⁶ Doe Run Dolomite Derby Dolomite Davis Formation Bonnetterre Dolomite ⁶ Reagan Sandstone Lamotte Sandstone	St. Peter Sandstone Everton Formation Smithville Formation Powell Dolomite			
		Van Buren Formation ⁴								
		Gunter Sandstone								
		Member ⁴								
		Eminence Dolomite								
		Potosi Dolomite								
		Doe Run Dolomite								
		Derby Dolomite								
		Davis Formation								
		Bonnetterre Formation ⁶								
Reagan Sandstone ⁴										
Lamotte Sandstone										
		Gasconade Dolomite	Kimmiswick Limestone			Cotter Dolomite Jefferson City Dolomite Roubidoux Formation Gasconade Dolomite Van Buren Formation ⁴ Gunter Sandstone Member ⁴ Eminence Dolomite Potosi Dolomite ⁶ Doe Run Dolomite Derby Dolomite Davis Formation Bonnetterre Dolomite ⁶ Reagan Sandstone Lamotte Sandstone	St. Peter Sandstone Everton Formation Smithville Formation Powell Dolomite			
		Van Buren Formation ⁴								
		Gunter Sandstone								
		Member ⁴								
		Eminence Dolomite								
		Potosi Dolomite								
		Doe Run Dolomite								
		Derby Dolomite								
		Davis Formation								
		Bonnetterre Formation ⁶								
Reagan Sandstone ⁴										
Lamotte Sandstone										
		Gasconade Dolomite	Kimmiswick Limestone			Cotter Dolomite Jefferson City Dolomite Roubidoux Formation Gasconade Dolomite Van Buren Formation ⁴ Gunter Sandstone Member ⁴ Eminence Dolomite Potosi Dolomite ⁶ Doe Run Dolomite Derby Dolomite Davis Formation Bonnetterre Dolomite ⁶ Reagan Sandstone Lamotte Sandstone	St. Peter Sandstone Everton Formation Smithville Formation Powell Dolomite			
		Van Buren Formation ⁴								
		Gunter Sandstone								
		Member ⁴								
		Eminence Dolomite								
		Potosi Dolomite								
		Doe Run Dolomite								
		Derby Dolomite								
		Davis Formation								
		Bonnetterre Formation ⁶								
Reagan Sandstone ⁴										
Lamotte Sandstone										
		Gasconade Dolomite	Kimmiswick Limestone			Cotter Dolomite Jefferson City Dolomite Roubidoux Formation Gasconade Dolomite Van Buren Formation ⁴ Gunter Sandstone Member ⁴ Eminence Dolomite Potosi Dolomite ⁶ Doe Run Dolomite Derby Dolomite Davis Formation Bonnetterre Dolomite ⁶ Reagan Sandstone Lamotte Sandstone	St. Peter Sandstone Everton Formation Smithville Formation Powell Dolomite			
		Van Buren Formation ⁴								
		Gunter Sandstone								
		Member ⁴								
		Eminence Dolomite								
		Potosi Dolomite								
		Doe Run Dolomite								
		Derby Dolomite								
		Davis Formation								
		Bonnetterre Formation ⁶								
Reagan Sandstone ⁴										
Lamotte Sandstone										
		Gasconade Dolomite	Kimmiswick Limestone			Cotter Dolomite Jefferson City Dolomite Roubidoux Formation Gasconade Dolomite Van Buren Formation ⁴ Gunter Sandstone Member ⁴ Eminence Dolomite Potosi Dolomite ⁶ Doe Run Dolomite Derby Dolomite Davis Formation Bonnetterre Dolomite ⁶ Reagan Sandstone Lamotte Sandstone	St. Peter Sandstone Everton Formation Smithville Formation Powell Dolomite			
		Van Buren Formation ⁴								
		Gunter Sandstone								
		Member ⁴								
		Eminence Dolomite								
		Potosi Dolomite								
		Doe Run Dolomite								
		Derby Dolomite								
		Davis Formation								
		Bonnetterre Formation ⁶								
Reagan Sandstone ⁴										
Lamotte Sandstone										
		Gasconade Dolomite	Kimmiswick Limestone			Cotter Dolomite Jefferson City Dolomite Roubidoux Formation Gasconade Dolomite Van Buren Formation ⁴ Gunter Sandstone Member ⁴ Eminence Dolomite Potosi Dolomite ⁶ Doe Run Dolomite Derby Dolomite Davis Formation Bonnetterre Dolomite ⁶ Reagan Sandstone Lamotte Sandstone	St. Peter Sandstone Everton Formation Smithville Formation Powell Dolomite			
		Van Buren Formation ⁴								
		Gunter Sandstone								
		Member ⁴								
		Eminence Dolomite								
		Potosi Dolomite								
		Doe Run Dolomite								
		Derby Dolomite								
		Davis Formation								
		Bonnetterre Formation ⁶								
Reagan Sandstone ⁴										
Lamotte Sandstone										
		Gasconade Dolomite	Kimmiswick Limestone			Cotter Dolomite Jefferson City Dolomite Roubidoux Formation Gasconade Dolomite Van Buren Formation ⁴ Gunter Sandstone Member ⁴ Eminence Dolomite Potosi Dolomite ⁶ Doe Run Dolomite Derby Dolomite Davis Formation Bonnetterre Dolomite ⁶ Reagan Sandstone Lamotte Sandstone	St. Peter Sandstone Everton Formation Smithville Formation Powell Dolomite			
		Van Buren Formation ⁴								
		Gunter Sandstone								
		Member ⁴								
		Eminence Dolomite								
		Potosi Dolomite								
		Doe Run Dolomite								
		Derby Dolomite								
		Davis Formation								
		Bonnetterre Formation ⁶								
Reagan Sandstone ⁴										
Lamotte Sandstone										
		Gasconade Dolomite	Kimmiswick Limestone			Cotter Dolomite Jefferson City Dolomite Roubidoux Formation Gasconade Dolomite Van Buren Formation ⁴ Gunter Sandstone Member ⁴ Eminence Dolomite Potosi Dolomite ⁶ Doe Run Dolomite Derby Dolomite Davis Formation Bonnetterre Dolomite ⁶ Reagan Sandstone Lamotte Sandstone	St. Peter Sandstone Everton Formation Smithville Formation Powell Dolomite			
		Van Buren Formation ⁴								
		Gunter Sandstone								
		Member ⁴								
		Eminence Dolomite								
		Potosi Dolomite								
		Doe Run Dolomite								
		Derby Dolomite								
		Davis Formation								
		Bonnetterre Formation ⁶								
Reagan Sandstone ⁴										
Lamotte Sandstone										
		Gasconade Dolomite	Kimmiswick Limestone			Cotter Dolomite Jefferson City Dolomite Roubidoux Formation Gasconade Dolomite Van Buren Formation ⁴ Gunter Sandstone Member ⁴ Eminence Dolomite Potosi Dolomite ⁶ Doe Run Dolomite Derby Dolomite Davis Formation Bonnetterre Dolomite ⁶ Reagan Sandstone Lamotte Sandstone	St. Peter Sandstone Everton Formation Smithville Formation Powell Dolomite			
		Van Buren Formation ⁴								
		Gunter Sandstone								
		Member ⁴								
		Eminence Dolomite								
		Potosi Dolomite								
		Doe Run Dolomite								
		Derby Dolomite								
		Davis Formation								
		Bonnetterre Formation ⁶								
Reagan Sandstone ⁴										
Lamotte Sandstone										
		Gasconade Dolomite	Kimmiswick Limestone			Cotter Dolomite Jefferson City Dolomite Roubidoux Formation Gasconade Dolomite Van Buren Formation ⁴ Gunter Sandstone Member ⁴ Eminence Dolomite Potosi Dolomite ⁶ Doe Run Dolomite Derby Dolomite Davis Formation Bonnetterre Dolomite ⁶ Reagan Sandstone Lamotte Sandstone	St. Peter Sandstone Everton Formation Smithville Formation Powell Dolomite			
		Van Buren Formation ⁴								
		Gunter Sandstone								
		Member ⁴								
		Eminence Dolomite								
		Potosi Dolomite								
		Doe Run Dolomite								
		Derby Dolomite								
		Davis Formation								
		Bonnetterre Formation ⁶								
Reagan Sandstone ⁴										
Lamotte Sandstone										
		Gasconade Dolomite	Kimmiswick Limestone			Cotter Dolomite Jefferson City Dolomite Roubidoux Formation Gasconade Dolomite Van Buren Formation ⁴ Gunter Sandstone Member ⁴ Eminence Dolomite Potosi Dolomite ⁶ Doe Run Dolomite Derby Dolomite Davis Formation Bonnetterre Dolomite ⁶ Reagan Sandstone Lamotte Sandstone	St. Peter Sandstone Everton Formation Smithville Formation Powell Dolomite			
		Van Buren Formation ⁴								
		Gunter Sandstone								
		Member ⁴								
		Eminence Dolomite								
		Potosi Dolomite								
		Doe Run Dolomite								
		Derby Dolomite								
		Davis Formation								
		Bonnetterre Formation ⁶								
Reagan Sandstone ⁴										
Lamotte Sandstone										
		Gasconade Dolomite	Kimmiswick Limestone			Cotter Dolomite Jefferson City Dolomite Roubidoux Formation Gasconade Dolomite Van Buren Formation ⁴ Gunter Sandstone Member ⁴ Eminence Dolomite Potosi Dolomite ⁶ Doe Run Dolomite Derby Dolomite Davis Formation Bonnetterre Dolomite ⁶ Reagan Sandstone Lamotte Sandstone	St. Peter Sandstone Everton Formation Smithville Formation Powell Dolomite			
		Van Buren Formation ⁴								
		Gunter Sandstone								
		Member ⁴								
		Eminence Dolomite								
		Potosi Dolomite								
		Doe Run Dolomite								
		Derby Dolomite								
		Davis Formation								
		Bonnetterre Formation ⁶								
Reagan Sandstone ⁴										
Lamotte Sandstone										
		Gasconade Dolomite	Kimmiswick Limestone			Cotter Dolomite Jefferson City Dolomite Roubidoux Formation Gasconade Dolomite Van Buren Formation ⁴ Gunter Sandstone Member ⁴ Eminence Dolomite Potosi Dolomite ⁶ Doe Run Dolomite Derby Dolomite Davis Formation Bonnetterre Dolomite ⁶ Reagan Sandstone Lamotte Sandstone	St. Peter Sandstone Everton Formation Smithville Formation Powell Dolomite			
		Van Buren Formation ⁴								
		Gunter Sandstone								
		Member ⁴								
		Eminence Dolomite								
		Potosi Dolomite								
		Doe Run Dolomite								
		Derby Dolomite								
		Davis Formation								
		Bonnetterre Formation ⁶								
Reagan Sandstone ⁴										
Lamotte Sandstone										
		Gasconade Dolomite	Kimmiswick Limestone			Cotter Dolomite Jefferson City Dolomite Roubidoux Formation Gasconade Dolomite Van Buren Formation ⁴ Gunter Sandstone Member ⁴ Eminence Dolomite Potosi Dolomite ⁶ Doe Run Dolomite Derby Dolomite Davis Formation Bonnetterre Dolomite ⁶ Reagan Sandstone Lamotte Sandstone	St. Peter Sandstone Everton Formation Smithville Formation Powell Dolomite			
		Van Buren Formation ⁴								
		Gunter Sandstone								
		Member ⁴								
		Eminence Dolomite								
		Potosi Dolomite								
		Doe Run Dolomite								
		Derby Dolomite								
		Davis Formation								
		Bonnetterre Formation ⁶								
Reagan Sandstone ⁴										
Lamotte Sandstone										
		Gasconade Dolomite	Kimmiswick Limestone			Cotter Dolomite Jefferson City Dolomite Roubidoux Formation Gasconade Dolomite Van Buren Formation ⁴ Gunter Sandstone Member ⁴ Eminence Dolomite Potosi Dolomite ⁶ Doe Run Dolomite Derby Dolomite Davis Formation Bonnetterre Dolomite ⁶ Reagan Sandstone Lamotte Sandstone	St. Peter Sandstone Everton Formation Smithville Formation Powell Dolomite			
		Van Buren Formation ⁴								
		Gunter Sandstone								
		Member ⁴								
		Eminence Dolomite								
		Potosi Dolomite								
		Doe Run Dolomite								
		Derby Dolomite								
		Davis Formation								
		Bonnetterre Formation ⁶								
Reagan Sandstone ⁴										
Lamotte Sandstone										
		Gasconade Dolomite	Kimmiswick Limestone			Cotter Dolomite Jefferson City Dolomite Roubidoux Formation Gasconade Dolomite Van Buren Formation ⁴ Gunter Sandstone Member ⁴ Eminence Dolomite Potosi Dolomite ⁶ Doe Run Dolomite Derby Dolomite Davis Formation Bonnetterre Dolomite ⁶ Reagan Sandstone Lamotte Sandstone	St. Peter Sandstone Everton Formation Smithville Formation Powell Dolomite			
		Van Buren Formation ⁴								
		Gunter Sandstone								
		Member ⁴								
		Eminence Dolomite								
		Potosi Dolomite								
		Doe Run Dolomite								
		Derby Dolomite								
		Davis Formation								
		Bonnetterre Formation ⁶								
Reagan Sandstone ⁴										
Lamotte Sandstone										
		Gasconade Dolomite	Kimmiswick Limestone			Cotter Dolomite Jefferson City Dolomite Roubidoux Formation Gasconade Dolomite Van Buren Formation ⁴ Gunter Sandstone Member ⁴ Eminence Dolomite Potosi Dolomite ⁶ Doe Run Dolomite Derby Dolomite Davis Formation Bonnetterre Dolomite ⁶ Reagan Sandstone Lamotte Sandstone	St. Peter Sandstone Everton Formation Smithville Formation Powell Dolomite			
		Van Buren Formation ⁴								
		Gunter Sandstone								
		Member ⁴								
		Eminence Dolomite								
		Potosi Dolomite								
		Doe Run Dolomite								
		Derby Dolomite								
		Davis Formation								
		Bonnetterre Formation ⁶								
Reagan Sandstone ⁴										
Lamotte Sandstone										
		Gasconade Dolomite	Kimmiswick Limestone			Cotter Dolomite Jefferson City Dolomite Roubidoux Formation Gasconade Dolomite Van Buren Formation ⁴ Gunter Sandstone Member ⁴ Eminence Dolomite Potosi Dolomite ⁶ Doe Run Dolomite Derby Dolomite Davis Formation Bonnetterre Dolomite ⁶ Reagan Sandstone Lamotte Sandstone	St. Peter Sandstone Everton Formation Smithville Formation Powell Dolomite			
		Van Buren Formation ⁴								
		Gunter Sandstone								
		Member ⁴								
		Eminence Dolomite								
		Potosi Dolomite								
		Doe Run Dolomite								
		Derby Dolomite								
		Davis Formation								
		Bonnetterre Formation ⁶								
Reagan Sandstone ⁴										
Lamotte Sandstone										
		Gasconade Dolomite	Kimmiswick Limestone			Cotter Dolomite Jefferson City Dolomite Roubidoux Formation Gasconade Dolomite Van Buren Formation ⁴ Gunter Sandstone Member ⁴ Eminence Dolomite Potosi Dolomite ⁶ Doe Run Dolomite Derby Dolomite Davis Formation Bonnetterre Dolomite ⁶ Reagan Sandstone Lamotte Sandstone	St. Peter Sandstone Everton Formation Smithville Formation Powell Dolomite			
		Van Buren Formation ⁴								
		Gunter Sandstone								
		Member ⁴								
		Eminence Dolomite								
		Potosi Dolomite								
		Doe Run Dolomite								
		Derby Dolomite								
		Davis Formation								
		Bonnetterre Formation ⁶								
Reagan Sandstone ⁴										
Lamotte Sandstone										
		Gasconade Dolomite	Kimmiswick Limestone			Cotter Dolomite Jefferson City Dolomite Roubidoux Formation Gasconade Dolomite Van Buren Formation ⁴ Gunter Sandstone Member ⁴ Eminence Dolomite Potosi Dolomite ⁶ Doe Run Dolomite Derby Dolomite Davis Formation Bonnetterre Dolomite ⁶ Reagan Sandstone Lamotte Sandstone	St. Peter Sandstone Everton Formation Smithville Formation Powell Dolomite			
		Van Buren Formation ⁴								
		Gunter Sandstone								
		Member ⁴								
		Eminence Dolomite								
		Potosi Dolomite								
		Doe Run Dolomite								
		Derby Dolomite								
		Davis Formation								
		Bonnetterre Formation ⁶								
Reagan Sandstone ⁴										
Lamotte Sandstone										
		Gasconade Dolomite	Kimmiswick Limestone			Cotter Dolomite Jefferson City Dolomite Roubidoux Formation Gasconade Dolomite Van Buren Formation ⁴ Gunter Sandstone Member ⁴ Eminence Dolomite Potosi Dolomite ⁶ Doe Run Dolomite Derby Dolomite Davis Formation Bonnetterre Dolomite ⁶ Reagan Sandstone Lamotte Sandstone	St. Peter Sandstone Everton Formation Smithville Formation Powell Dolomite			
		Van Buren Formation ⁴								
		Gunter Sandstone								
		Member ⁴								
		Eminence Dolomite								
		Potosi Dolomite								
		Doe Run Dolomite								
		Derby Dolomite								
		Davis Formation								
		Bonnetterre Formation ⁶								
Reagan Sandstone ⁴										
Lamotte Sandstone										
		Gasconade Dolomite	Kimmiswick Limestone			Cotter Dolomite Jefferson City Dolomite Roubidoux Formation Gasconade Dolomite Van Buren Formation ⁴ Gunter Sandstone Member ⁴ Eminence Dolomite Potosi Dolomite ⁶ Doe Run Dolomite Derby Dolomite Davis Formation Bonnetterre Dolomite ⁶ Reagan Sandstone Lamotte Sandstone	St. Peter Sandstone Everton Formation Smithville Formation Powell Dolomite			
		Van Buren Formation ⁴								
		Gunter Sandstone								
		Member ⁴								
		Eminence Dolomite								
		Potosi Dolomite								
		Doe Run Dolomite								
		Derby Dolomite								
		Davis Formation								
		Bonnetterre Formation ⁶								
Reagan Sandstone ⁴										
Lamotte Sandstone										
		Gasconade Dolomite	Kimmiswick Limestone			Cotter Dolomite Jefferson City Dolomite Roubidoux Formation Gasconade Dolomite Van Buren Formation ⁴ Gunter Sandstone Member ⁴ Eminence Dolomite Potosi Dolomite ⁶ Doe Run Dolomite Derby Dolomite Davis Formation Bonnetterre Dolomite ⁶ Reagan Sandstone Lamotte Sandstone	St. Peter Sandstone Everton Formation Smithville Formation Powell Dolomite			
		Van Buren Formation ⁴								
		Gunter Sandstone								
		Member ⁴								
		Eminence Dolomite								
		Potosi Dolomite								
		Doe Run Dolomite								
		Derby Dolomite								
		Davis Formation								
		Bonnetterre Formation ⁶								
Reagan Sandstone ⁴										
Lamotte Sandstone										
		Gasconade Dolomite	Kimmiswick Limestone			Cotter Dolomite Jefferson City Dolomite Roubidoux Formation Gasconade Dolomite Van Buren Formation ⁴ Gunter Sandstone Member ⁴ Eminence Dolomite Potosi Dolomite ⁶ Doe Run Dolomite Derby Dolomite Davis Formation Bonnetterre Dolomite ⁶ Reagan Sandstone Lamotte Sandstone	St. Peter Sandstone Everton Formation Smithville Formation Powell Dolomite			
		Van Buren Formation ⁴								
		Gunter Sandstone								
		Member ⁴								
		Eminence Dolomite								
		Potosi Dolomite								
		Doe Run Dolomite								
		Derby Dolomite								
		Davis Formation								
		Bonnetterre Formation ⁶								
Reagan Sandstone ⁴										
Lamotte Sandstone										
		Gasconade Dolomite	Kimmiswick Limestone			Cotter Dolomite Jefferson City Dolomite Roubidoux Formation Gasconade Dolomite Van Buren Formation ⁴ Gunter Sandstone Member ⁴ Eminence Dolomite Potosi Dolomite ⁶ Doe Run Dolomite Derby Dolomite Davis Formation Bonnetterre Dolomite ⁶ Reagan Sandstone Lamotte Sandstone	St. Peter Sandstone Everton Formation Smithville Formation Powell Dolomite			
		Van Buren Formation ⁴								
		Gunter Sandstone								
		Member ⁴								
		Eminence Dolomite								
		Potosi Dolomite								
		Doe Run Dolomite								
		Derby Dolomite								
		Davis Formation								
		Bonnetterre Formation ⁶								
Reagan Sandstone ⁴										
Lamotte Sandstone										
		Gasconade Dolomite	Kimmiswick Limestone			Cotter Dolomite Jefferson City Dolomite Roubidoux Formation Gasconade Dolomite Van Buren Formation ⁴ Gunter Sandstone Member ⁴ Eminence Dolomite Potosi Dolomite ⁶ Doe Run Dolomite Derby Dolomite Davis Formation Bonnetterre Dolomite ⁶ Reagan Sandstone Lamotte Sandstone	St. Peter Sandstone Everton Formation Smithville Formation Powell Dolomite			
		Van Buren Formation ⁴								
		Gunter Sandstone								
		Member ⁴								
		Eminence Dolomite								
		Potosi Dolomite								
		Doe Run Dolomite								
		Derby Dolomite								
		Davis Formation								
		Bonnetterre Formation ⁶								
Reagan Sandstone ⁴										
Lamotte Sandstone										
		Gasconade Dolomite	Kimmiswick Limestone			Cotter Dolomite Jefferson City Dolomite Roubidoux Formation Gasconade Dolomite Van Buren Formation ⁴ Gunter Sandstone Member ⁴ Eminence Dolomite Potosi Dolomite ⁶ Doe Run Dolomite Derby Dolomite Davis Formation Bonnetterre Dolomite ⁶ Reagan Sandstone Lamotte Sandstone	St. Peter Sandstone Everton Formation Smithville Formation Powell Dolomite			
		Van Buren Formation ⁴								
		Gunter Sandstone								
		Member ⁴								
		Eminence Dolomite								
		Potosi Dolomite								
		Doe Run Dolomite								
		Derby Dolomite								
		Davis Formation								
		Bonnetterre Formation ⁶								
Reagan Sandstone ⁴										
Lamotte Sandstone										
		Gasconade Dolomite	Kimmiswick Limestone			Cotter Dolomite Jefferson City Dolomite Roubidoux Formation Gasconade Dolomite Van Buren Formation ⁴ Gunter Sandstone Member ⁴ Eminence Dolomite Potosi Dolomite ⁶ Doe Run Dolomite Derby Dolomite Davis Formation Bonnetterre Dolomite ⁶ Reagan Sandstone Lamotte Sandstone	St. Peter Sandstone Everton Formation Smithville Formation Powell Dolomite			
		Van Buren Formation ⁴								
		Gunter Sandstone								
		Member ⁴								
		Eminence Dolomite								
		Potosi Dolomite								
		Doe Run Dolomite								
		Derby Dolomite								
		Davis Formation								
		Bonnetterre Formation ⁶								
Reagan Sandstone ⁴										
Lamotte Sandstone										
		Gasconade Dolomite	Kimmiswick Limestone			Cotter Dolomite Jefferson City Dolomite Roubidoux Formation Gasconade Dolomite Van Buren Formation ⁴ Gunter Sandstone Member ⁴ Eminence Dolomite Potosi Dolomite ⁶ Doe Run Dolomite Derby Dolomite Davis Formation Bonnetterre Dolomite ⁶ Reagan Sandstone Lamotte Sandstone	St. Peter Sandstone Everton Formation Smithville Formation Powell Dolomite			
		Van Buren Formation ⁴								
		Gunter Sandstone								
		Member ⁴								
		Eminence Dolomite								
		Potosi Dolomite								
		Doe Run Dolomite								
		Derby								

¹Geologic unit in southeastern Missouri that is stratigraphically equivalent to geologic units in the Western Interior Plains confining system but not part of the confining system.

²The Western Interior Plains confining system also includes younger sediments west of the study area.

³Geologic unit in southeastern Missouri that is stratigraphically equivalent to geologic units in the Springfield Plateau aquifer but not part of the aquifer.

⁴Unit follows usage of the Missouri Division of Geology and Land Survey.

⁵The Western Interior Plains aquifer system deeply buried in the western part of the study area included where permeable carbonate rocks in the subsurface are equivalents of the aquifers of the Ozark Plateaus aquifer system (Miller and Appel, 1997).

system (Miller and Appel, 1997).

⁶Unit follows usage of the National Geologic Map database.

Figure 2. Generalized correlation of Paleozoic units and regional hydrogeologic units of the Ozark Plateaus aquifer system with corresponding model layer number. Modified from Hays and others (2016).—Continued.

model stresses and parameters are modified to better fit historical hydraulic-head (groundwater-level altitude) and stream-leakage data (flow into or out of a stream relative to the aquifer system). A hydraulic property value for each model cell is interpolated based on the corresponding property values of the surrounding pilot points. This process allows for spatial variation of hydraulic properties to be represented in a gradational manner rather than applying hydraulic property values to discrete zones in the model. More information on geostatistical methods and the use of pilot points is available in Doherty (2011). Pilot points were distributed uniformly across the model area at a spacing of approximately 15 miles (mi) (fig. 3) within the active area constraints of each model layer. Generally, pilot-point parameters were named based on a sequential number, an abbreviated form of the hydraulic property represented by the point, and the corresponding model layer, if applicable. Additional parameters were specified as multipliers on boundaries and stresses to acknowledge uncertainty in the model input, and so that the sensitivity and identifiability of the model input could be better quantified.

Because information and model development may change through time, the model documented in this report is considered version 1.0. In some instances, such as the temporal discretization, information from previous investigations was used as a basis for the model (Richards, 2010). Several recent publications contain information pertinent to the construction of the Ozark model. Knierim and others (2015) compiled seepage-run data from 15 studies within the model area. Nottmeier (2015) documented a regional potentiometric map of the Ozark aquifer. Knierim and others (2016, 2017) created a site-specific groundwater use record for the Ozark system. Westerman and others (2016a, b) developed the altitudes and thicknesses of the hydrogeologic units used in the model.

Spatial Discretization and Layering

The finite-difference grid is oriented north-south and consists of 324 rows, 335 columns, and 9 layers with over 473,000 active cells. Though a single model layer of the rectangular finite-difference grid contains over 108,000 cells, many cells are inactive because they fall outside the active model area. Cells are a uniform 1 mi² (1 mi on a side) with varying thickness by layer. The northwestern corner of the grid is located at a latitude of 39°27'55.56" N and a longitude of 95°30'15.90" W. Vertically, the hydrogeologic units are discretized into 9 model layers (fig. 2). Spatially, each unit generally extends to the exterior boundary of the model area, though younger units have been eroded away in a concentric fashion from the outcrop of the basement unit (fig. 1) (Westerman and others, 2016b). Where the upper Ozark aquifer is not present, the properties of layer 4 are assigned the values of the underlying unit. The thickness of layer 4 also is modified to maintain a 1-ft minimum thickness. This was enforced to accommodate the requirement of continuous model layers throughout the finite-difference grid of the model.

Temporal Discretization

The simulation period extends from January 1, 1900, to April 1, 2016, for a total of 116 years and 79 stress periods (table 1). The first stress period is simulated as steady state to represent predevelopment conditions; no pumping is specified in stress period 1. The transient stress periods following the initial steady-state period gradually increase in length to correspond to an increase in spatial and temporal information about the system, particularly head observations and pumping. Stress period 2 represents the time period from 1900 through 1939, and stress period 3 represents the time period from 1940 through 1964, both indicating a period where relatively little pumping information is recorded. Stress periods 4 through 28 are each 1 year in length, representing the time period from 1965 through 1989. Stress period 29 is 455 days in length to encompass the full year of 1990 and the spring (January through March) of 1991. These stress period lengths allow variations in groundwater pumping annually as demand changes with time. Stress periods 30 through 79 are each 6 months in length—April through September (representing spring and summer) and October through March (representing fall and winter) to encompass the later part of 1991 to 2015. The 6-month stress period lengths correspond to variations in groundwater pumping that occurs on a semiseasonal basis reported by Wittman and others (2003) in southwestern Missouri and presumably occur across the model area in a similar fashion. Semiseasonal stress periods represent higher demand and lower recharge in the spring and summer months and lower demand and higher recharge in the fall and winter months.

The digital archive of the model includes an additional stress period at the end of the simulation. This stress period is simulated as steady state and was included for preliminary evaluation of forecast uncertainty. A detailed discussion of forecast uncertainty is beyond the purpose of this report, and the final stress period and associated forecast observations are not included as part of this report.

Areal Recharge

Areal recharge is applied to the highest active model cells throughout the Ozark model area by using the MODFLOW-NWT Recharge (RCH) Package (Niswonger and others, 2011; Harbaugh, 2005). Recharge to the Ozark system aquifers is dominated by meteoric water not lost to evapotranspiration, interception by plants, or runoff to land surfaces outside the study area boundaries (Hays and others, 2016). Initial estimates of recharge were determined from the Soil-Water Balance (SWB) model, which uses inputs of tabular and gridded datasets of precipitation and air temperature, hydrologic soil groups, available soil-water capacity, and land-use and land-cover data (Westenbroek and others, 2010). Approximately 24 percent of the precipitation from 2005 through 2014 recharged the Ozark system, and

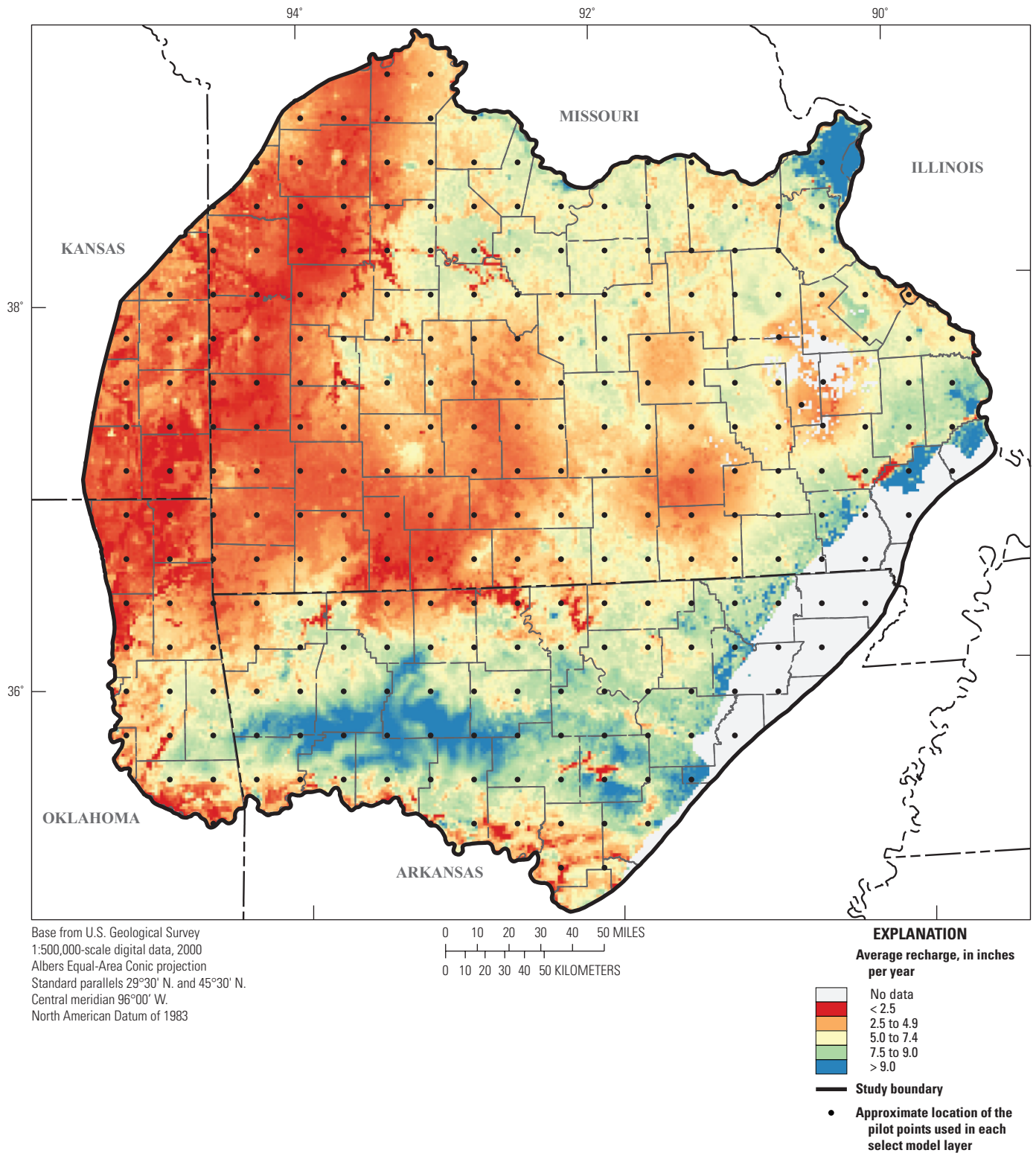


Figure 3. Pilot-point distribution with final calibrated values of average, model adjusted recharge from 2000 to 2013.

Table 1. Stress period discretization used in the Ozark model.

[Mgal/d, million gallons per day; in/yr, inch per year; SS, steady state; TR, transient]

Stress period	Begin date	Number of days	Cumulative days	Stress period type	Specified pumping (Mgal/d)	Average recharge (in/yr)	Stress period	Begin date	Number of days	Cumulative days	Stress period type	Specified pumping (Mgal/d)	Average recharge (in/yr)
1	1/1/1900	1	1	SS	0	3.75	41	10/1/1996	182	35,520	TR	107.87	8.04
2	1/2/1900	14,609	14,610	TR	30.43	3.67	42	4/1/1997	183	35,703	TR	444.57	0.93
3	1/1/1940	9,132	23,742	TR	84.86	3.55	43	10/1/1997	182	35,885	TR	109.48	7.44
4	1/1/1965	365	24,107	TR	142.13	3.75	44	4/1/1998	183	36,068	TR	468.99	1.27
5	1/1/1966	365	24,472	TR	148.38	3.23	45	10/1/1998	182	36,250	TR	111.95	5.01
6	1/1/1967	365	24,837	TR	151.68	3.63	46	4/1/1999	183	36,433	TR	503.79	1.80
7	1/1/1968	366	25,203	TR	155.60	4.11	47	10/1/1999	183	36,616	TR	117.88	2.50
8	1/1/1969	365	25,568	TR	156.06	3.71	48	4/1/2000	183	36,799	TR	540.00	1.17
9	1/1/1970	365	25,933	TR	160.46	3.75	49	10/1/2000	182	36,981	TR	124.28	5.77
10	1/1/1971	365	26,298	TR	167.99	3.11	50	4/1/2001	183	37,164	TR	538.01	0.61
11	1/1/1972	366	26,664	TR	172.51	3.67	51	10/1/2001	182	37,346	TR	123.61	6.71
12	1/1/1973	365	27,029	TR	177.61	5.07	52	4/1/2002	183	37,529	TR	540.58	2.49
13	1/1/1974	365	27,394	TR	182.77	4.03	53	10/1/2002	182	37,711	TR	124.41	4.20
14	1/1/1975	365	27,759	TR	189.21	3.99	54	4/1/2003	183	37,894	TR	546.94	1.70
15	1/1/1976	366	28,125	TR	194.70	2.71	55	10/1/2003	183	38,077	TR	126.47	5.76
16	1/1/1977	365	28,490	TR	200.60	3.87	56	4/1/2004	183	38,260	TR	562.65	1.72
17	1/1/1978	365	28,855	TR	206.30	3.67	57	10/1/2004	182	38,442	TR	131.66	8.04
18	1/1/1979	365	29,220	TR	211.90	3.79	58	4/1/2005	183	38,625	TR	568.97	0.91
19	1/1/1980	366	29,586	TR	219.77	2.47	59	10/1/2005	182	38,807	TR	133.71	2.55
20	1/1/1981	365	29,951	TR	224.67	3.87	60	4/1/2006	183	38,990	TR	581.91	1.44
21	1/1/1982	365	30,316	TR	230.26	4.71	61	10/1/2006	182	39,172	TR	138.80	7.50
22	1/1/1983	365	30,681	TR	233.27	3.99	62	4/1/2007	183	39,355	TR	583.68	1.47
23	1/1/1984	366	31,047	TR	236.14	4.27	63	10/1/2007	183	39,538	TR	138.97	7.83
24	1/1/1985	365	31,412	TR	240.30	5.03	64	4/1/2008	183	39,721	TR	589.78	4.93
25	1/1/1986	365	31,777	TR	243.17	3.95	65	10/1/2008	182	39,903	TR	140.59	3.75
26	1/1/1987	365	32,142	TR	249.10	3.91	66	4/1/2009	183	40,086	TR	599.17	3.74
27	1/1/1988	366	32,508	TR	249.56	3.63	67	10/1/2009	182	40,268	TR	143.31	8.92
28	1/1/1989	365	32,873	TR	253.78	3.03	68	4/1/2010	183	40,451	TR	618.39	2.64
29	1/1/1990	455	33,328	TR	110.44	5.44	69	10/1/2010	182	40,633	TR	149.31	4.17
30	4/1/1991	183	33,511	TR	400.27	1.60	70	4/1/2011	183	40,816	TR	618.39	4.17
31	10/1/1991	183	33,694	TR	108.25	5.46	71	10/1/2011	183	40,999	TR	149.31	6.57
32	4/1/1992	183	33,877	TR	396.29	0.95	72	4/1/2012	183	41,182	TR	618.39	0.69
33	10/1/1992	182	34,059	TR	106.37	8.23	73	10/1/2012	182	41,364	TR	149.31	4.94
34	4/1/1993	183	34,242	TR	391.26	3.76	74	4/1/2013	183	41,547	TR	618.39	3.18
35	10/1/1993	182	34,424	TR	104.13	6.48	75	10/1/2013	182	41,729	TR	149.31	4.76
36	4/1/1994	183	34,607	TR	390.90	2.01	76	4/1/2014	183	41,912	TR	618.39	1.41
37	10/1/1994	182	34,789	TR	103.46	6.09	77	10/1/2014	182	42,094	TR	149.31	5.96
38	4/1/1995	183	34,972	TR	391.58	2.74	78	4/1/2015	183	42,277	TR	618.39	4.02
39	10/1/1995	183	35,155	TR	103.13	3.20	79	10/1/2015	183	42,460	TR	149.31	5.96
40	4/1/1996	183	35,338	TR	422.75	2.34							

rates ranged from 0 (areas of open water) to 32 in/yr, with an average rate of 13.4 in/yr. Recharge results from the SWB model were within the range of reported values for the model area but generally higher than values calibrated during previous modeling efforts (Hays and others, 2016). Therefore, secondary estimates of recharge were calculated through annual regression-based methods, referred to as the Empirical Water Balance (EWB) (Reitz and others, 2015, 2017).

The EWB represents average recharge from 2000 to 2013 and incorporates remotely sensed data including land cover, precipitation, and air temperature. The method is calibrated to long-term water balance data from 679 watersheds across the Nation (Reitz and others, 2015, 2017). In order to transform the EWB average recharge rates into time-series values, a multiplier was applied to each model stress period to represent general temporal changes in precipitation from 1900 to 1990 (stress periods 1–29; table 1). Precipitation records from 20 stations across the study area were compiled, and the amounts were averaged by stress period to compute the fractional change from the average 2000 to 2013 EWB recharge, which provided the initial temporal multiplier values from 1900 to 1990. These temporal multipliers were then defined as individual parameters and allowed to change during the history-matching process. The temporal multipliers are a simplification of the changes in recharge that occur through time. Because evapotranspiration, antecedent conditions, and other factors that control recharge are not represented in these multipliers, they likely do not represent local conditions. However, the primary intent was to provide a mechanism to adjust large-scale wet and dry periods through the temporal multipliers.

A slightly different method was used to adjust recharge from 1990 to 2015, which is represented by one transitional stress period (29) and multiple 6-month stress periods in the model (stress periods 29–79, table 1). The average 1981–2015 (24-yr) recharge from the SWB model was divided into each model-associated 6-month period recharge in the SWB to compute a fractional change from the 24-yr average for each cell. These multipliers better represent temporal changes in recharge caused by variation in precipitation and evapotranspiration throughout the latter part of the simulation period. Predevelopment recharge was represented by averaging the data from all precipitation stations and computing the fractional change from average 2000 to 2013 EWB recharge to use as the recharge multiplier on stress period 1. Recharge was further modified spatially during the history-matching process through the use of pilot points.

Groundwater Pumpage

Site-specific groundwater-pumping rates for the Ozark system from 1900 to 2010 were estimated by using a combination of county-aggregate water-use data from the USGS (1985–2010) and site-specific water-use data from a variety of Federal and State sources (1962–2010) (Knierim

and others, 2016, 2017). Site-specific pumping data were only available for public supply and non-agricultural use (including thermoelectric power generation, industrial, commercial, and mining) with limited site-specific data for agricultural (including irrigation and aquaculture) and domestic use. No site-specific pumping data were available for the livestock water-use category. Therefore, the estimation of groundwater pumping from the Ozark system was challenging because of the paucity of water-use data prior to the mid-1900s (Knierim and others, 2016, 2017).

As described in Knierim and others (2016, 2017), groundwater pumping rates for domestic and public supply were estimated by using population as a predictive variable, which was scaled to 0 million gallons per day (Mgal/d) in 1900 by using a linear multiplier in order to not overestimate pumping prior to the 1950s. Groundwater pumping rates for the other water-use categories (agriculture, livestock, and nonagriculture) were estimated by using simple linear extrapolation from the last year of reported data (generally 1985) to 0 Mgal/d in 1900. The pumping dataset by Knierim and others (2016) was developed to (1) estimate groundwater pumping rates as accurately as possible, by relying on State-furnished site-specific data and by using USGS county-aggregated data as a quality-control check; (2) disaggregate county-level data (where site-specific data were unavailable) to individual wells; (3) attribute pumping to individual aquifers to realistically reflect the hydrogeology and overall water use from the system; and (4) estimate historical water use prior to the mid-1900s when few data were available. Estimates from the final dataset indicate that groundwater pumping rates increased from an estimated 0 Mgal/d in 1900 to 104 Mgal/d in 1950, and to 380 Mgal/d in 2010, with public supply constituting the largest portion of total groundwater use (Knierim and others, 2017).

Groundwater pumping estimated by Knierim and others (2016) was simulated in the groundwater-flow model by using the Well (WEL) Package (Harbaugh, 2005). To integrate the estimated site-specific dataset into the groundwater-flow model, pumping from wells within a single model cell were summed. Model row and column were determined through an intersection of the well coordinates with the spatially referenced model grid, and model layer was determined by comparing the altitude of the bottom of the well to the altitude of each hydrogeologic unit. For the year 2010, most groundwater use (55 percent) was from the lower Ozark aquifer, which also includes 57 percent of the wells (Knierim and others, 2017). Groundwater use from the middle Ozark aquifer in 2010 accounts for approximately 21 percent of the total use from 29 percent of the wells.

The estimated annual pumping (Knierim and others, 2016) was recomputed to correspond to the variable length model stress periods described in “Temporal Discretization.” Pumping amounts were unchanged for stress periods representing 1 year. For stress periods that extended across multiple years, annual pumping amounts were averaged to produce a single value for the stress period. For the 6-month

stress periods that represent seasonal changes in pumping, amounts were unchanged, increased, or decreased depending on the season and use of the water (agriculture, public supply, and others). Agricultural pumping was removed during fall/winter stress periods and doubled during spring/summer stress periods to better simulate the seasonality of agricultural pumping throughout the year. Other pumping uses were reduced by 50 percent during fall/winter stress periods and increased by 50 percent during spring/summer stress periods. Fifty percent was used as the estimate of seasonal pumpage adjustment based on the observations by Wittman and others (2003) who found that in southwestern Missouri most communities increased their pumping by 25–50 percent in the summer; some communities increased their pumpage by as much as three times their winter pumpage. During the history-matching process, simulated water levels in Ottawa County, Oklahoma, were consistently higher than observed water levels. Aquifer properties and total pumping amounts were compared to those within a local-scale model (Czarnecki and others, 2009) and adjusted accordingly, which translated to an approximate doubling of pumping in Ottawa County. A single multiplier was applied as a parameter to all pumping values throughout the simulation period.

Hydrologic Boundaries

Hydrologic boundaries determine the locations and quantities of simulated flow into and out of the model; therefore, the selection of appropriate boundaries for the model is a major concern in a modeling effort. The selection of model boundaries for the Ozark system is based on a conceptual interpretation of the flow system developed by using information reported by Imes and Emmett (1994) and Hays and others (2016).

Streams

Streams are represented as head-dependent flux boundaries by using the River (RIV) Package (Harbaugh, 2005). Streams simulated in the model are based on the National Hydrography Dataset (NHDPlus; McKay and others, 2012) and include those with a stream order greater than one (fig. 4). Initially, streambed hydraulic conductivities were specified as pilot-point parameters to be adjusted during the history-matching phase of the simulation. Streambed thickness was specified as 0.9 ft and assigned to the appropriate model layer based on the stream bottom altitude. Stream width within each model cell was estimated programmatically based on arbolate sum (total length of upstream drainage) by using the regression relation in Feinstein and others (2010). Stream length was determined by the NHDPlus stream length within each model cell. Streambed altitudes were based on 30-meter (m) digital elevation models (DEM) (U.S. Geological Survey, 2017a) and forced to decrease monotonically downstream (as inaccuracies

or the resolution of the DEM do not perfectly match the path of the stream). Though the Streamflow-Routing (SFR2) Package (Niswonger and Prudic, 2005) allows input for overland runoff to streams, this option was not used for the Ozark model because of the need to simulate only base-flow conditions and the evidence of a net flux of groundwater to surface water (Hays and others, 2016). Excessive model runtimes with the SFR2 Package precluded extensive exploration through parameter estimation; thus, the SFR2 package was converted to the RIV Package (Harbaugh, 2005) to reduce model runtime for much of the history-matching phase of model development. Stream bottom altitudes were used from previously developed SFR2 Packages. Because streams predominately act as a major discharge component of the groundwater system based on seepage data analysis and the hydrologic budget (Knierim and others, 2015, Hays and others, 2016), stream stage in the RIV package was set to zero to ensure streams act as discharge rather than recharge sources. Streams were grouped by 8-digit hydrologic unit code (U.S. Geological Survey, 2017b) to create 58 stream parameters used to modify the value of streambed conductance. These stream parameters represent multipliers that were applied to the initial streambed conductance values for each river cell within each hydrologic unit.

Specified-Head and No-Flow Boundaries

Streams and geological controls define Ozark system boundary extents. Lateral inflow is not volumetrically important to surface water or groundwater for the Ozark system because of an outward radial regional flow pattern. Lateral outflow from the Ozark system generally occurs in two locations—(1) in the southeastern part of the study area where the Ozark system underlies the Mississippi embayment regional aquifer system (MERAS; Clark and others, 2013), and (2) along the western edge of the study area where fresh groundwater mixes with saline groundwater that occurs down dip and forms the western boundary (Hays and others, 2016). The remaining model perimeter to the north-northeast and the south-southwest represents boundaries where flow into or out of the model area is assumed to be negligible (Hays and others, 2016) and is represented as a no-flow boundary. The base of the flow system (representing Precambrian-age basement rocks) is also represented as a no-flow boundary.

Boundaries other than no-flow boundaries were defined in the General-Head Boundary (GHB) and Constant-Head Boundary (CHD) Packages. Potential flow to and from the overlying MERAS in the southeastern part of the model area in parts of model layers 1–5 was represented by a GHB (Harbaugh, 2005). The specified-head values within the GHB were extracted from the simulation of the MERAS model (Clark and others, 2013) and represented simulated heads in 2006 to better approximate interaction between the two aquifer systems over recent decades. An initial conductance value of the GHB was specified

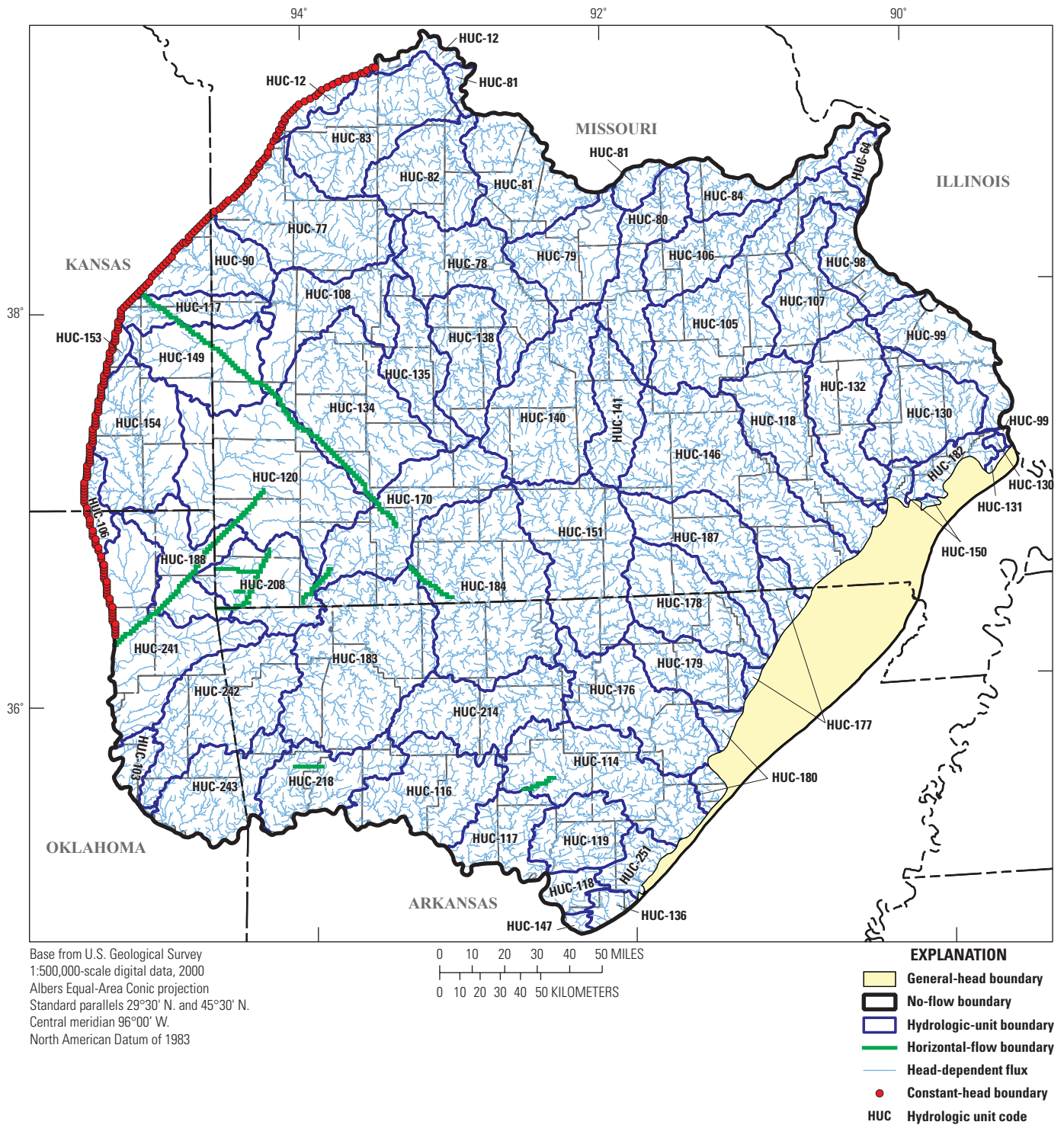


Figure 4. Head-dependent flux, specified head, and horizontal flow boundaries implemented in the Ozark model.

as 100 square feet per day (ft^2/d) to allow a reasonable fit to observed groundwater-level altitudes in the area. A single multiplier was applied to all GHB conductances as an adjustable parameter. The western edge of the model area is represented by a CHD (Harbaugh, 2005) in selected aquifer layers of the model (fig. 4). Specified heads in these layers were developed based on surrounding observed water levels and potentiometric surfaces (Nelson and others, 2015). A multiplier was applied to each layer containing CHD as a parameter to allow the altitude of the specified heads to slightly move up or down during the history-matching process.

Saline-Freshwater Interface

Groundwater of elevated salinity occurs along almost the entire boundary of the model area (Imes and Emmett, 1994) where the hydrogeologic units of the Ozark system occur at depth. For much of the model boundary, groundwater flow to and from these saline areas is assumed negligible (Imes and Emmett, 1994) and is represented as no-flow boundaries. However, an area in southwestern Missouri, northeastern Oklahoma, and southeastern Kansas has been of concern where groundwater near pumping centers contains elevated dissolved solids (Macfarlane and Hathaway, 1987; Czarnecki and others, 2009). Though a saline-freshwater interface is not simulated explicitly in the model, the CHD along the western edge of the model domain provides an indirect assessment of groundwater flow that may occur across the interface through the quantity of water simulated as leaving or entering the Ozark system.

Faults

Faulting is prevalent throughout the model area, and offset within and between hydrogeologic units can be from a few feet to several hundred feet or more (Imes and Emmett, 1994). At a local scale, faulting and karst conduits can route groundwater across surface-water hydrologic divides as evidenced by numerous dye-trace studies throughout the Ozark system (Hays and others, 2016); however, these past studies and existing data indicate little effect on groundwater flow at regional scales from the presence of faults (Imes, 1989). Because of this, few faults are simulated in the Ozark model; however, in some instances, the effect of faults on groundwater flow was evident where water-level altitudes indicated drastic differences over very short distances (hundreds of feet within one or two model cells), or the model simulation appeared to allow substantially more groundwater flow to areas than would be indicated by observation data. The Horizontal-Flow Boundary (HFB; Harbaugh, 2005) Package was used to restrict flow between model cells that occurred over short distances in the southern part of the model area and across long, regional faults in the southwestern part of the model area (fig. 4). A single multiplier was applied to the hydraulic characteristic of all HFBs as an adjustable parameter.

Hydraulic Properties

Hydraulic properties refer to the horizontal and vertical hydraulic conductivity and storage (specific yield and specific storage) values for each hydrogeologic unit within the Ozark model. The distribution of hydraulic properties in the model layers was represented as parameters through pilot points or uniform values for an entire layer. Initial values were assigned from previous modeling efforts (Imes and Emmett, 1994; Czarnecki and others, 2009; Richards, 2010), and from interpretations of pumping data and water-level response (Hays and others, 2016). Selected hydraulic properties and layers were assigned uniform values where prior information was sparse. Two areas of the model were assigned uniform values by layer, where appropriate, to represent alluvial sediments in the Mississippi embayment (Clark and others, 2013) and rocks stratigraphically equivalent to those represented in the model in the north-central part of the model area (fig 1). The Mississippi embayment area was assigned values of 350 feet per day (ft/d), 0.1 ft/d , 0.3, and 0.003 ft^{-1} representing horizontal hydraulic conductivity, vertical hydraulic conductivity, specific yield, and specific storage, respectively. The north-central rocks were assigned values of 0.32 and 0.1 ft/d for values of horizontal and vertical conductivity, respectively, based on similar hydraulic properties of equivalent stratigraphic units (Imes and Emmett, 1994). Specific storage and specific yield of the north-central rocks were the same value as the remainder of the associated layer.

Hydraulic Conductivity

Computed and previously simulated horizontal hydraulic conductivity values were available for parts of the Ozark aquifer, but values for the Springfield Plateau and St. Francois aquifers were scarce. In general, estimates of horizontal hydraulic conductivity range from 0.2 to 43 ft/d in the Springfield Plateau aquifer (layer 2), 8.64×10^{-4} to 86.4 ft/d in the Ozark aquifer (layers 4, 5, and 6), and 8.64×10^{-2} to 8.64 ft/d in the St. Francois aquifer (layers 8 and 9; Hays and others, 2016). Higher hydraulic conductivity values have been associated with the prevalence of karst conduits in the system, but these conduits typically occur over smaller spatial scales than are modeled with a regional groundwater-flow model. Some values of vertical hydraulic conductivity were available for the Western Interior Plains confining system, the Springfield Plateau aquifer, the Ozark confining unit, the Ozark aquifer, and the St. Francois aquifer (overall range from 9.0×10^{-9} to 1 ft/d) (Hays and others, 2016).

The known horizontal and vertical hydraulic conductivity values were used as initial values for pilot points in each hydrogeologic unit. Pilot-point values for the horizontal hydraulic conductivity of the aquifers represented by layers 2, 4, 6, and 9, and vertical hydraulic conductivity of confining units represented by layers 1, 3, 5, and 7 were then adjusted through the history-matching process. Vertical to horizontal

anisotropy of hydraulic conductivity for all layers was estimated to be 1:10. Model layers 8 and 9, representing the St. Francois aquifer, could not be independently calibrated because of the lack of observed water-level measurements in the St. Francois aquifer that could be attributed to a single layer of the model; thus, all hydraulic properties of layer 8 were set equal to the properties of layer 9.

Storage

Storage coefficients within the Ozark system are relatively low, typically less than 0.01 in the Ozark aquifer, even for unconfined conditions (Imes, 1989; Czarnecki and others, 2009; Richards, 2010; Hays and others, 2016). Though storage values in the Springfield Plateau aquifer may be slightly higher in some areas, the predominance of low storage and low hydraulic conductivity often creates large fluctuations in groundwater levels because of seasonal changes in recharge and pumping. Groundwater fluctuations of more than 100 ft, and occasionally more than 150 ft/yr, have been observed in observation wells in the Ozark system, particularly in areas of southwestern Missouri where the Ozark aquifer is primarily confined. Storage values in the Ozark model, both specific yield and specific storage, were represented as uniform values across all model layers except layer 6 and adjusted during the history-matching process. Pilot points were incorporated only for layer 6, the most productive part of the Ozark aquifer, for both specific yield and specific storage parameters.

Model History Matching

History matching is the process of changing model stresses and parameters to acceptably fit historical information such as hydraulic-head observations and stream-leakage estimates. History matching for the Ozark model was accomplished by a combination of manual changes to parameter values (primarily during early development) and automated calibration methods. Automated parameter estimation was achieved through the use of parameter estimation software (PEST; Doherty, 2010; Welter and others, 2015). PEST automatically adjusts input parameters (hydraulic conductivity, specific yield, specific storage, recharge, and riverbed conductance) in a series of model simulations. Many parameters were defined as pilot points, as described in “Groundwater-Flow Model Construction.” After each PEST process, simulated hydraulic-head values and stream leakage were compared to measured hydraulic head and stream leakage. The PEST simulations continued until the objective function (sum of the squared differences between simulated and measured values) could no longer be reduced. The history-matching approach used in this study differs from traditional nonlinear regression parameter estimation in two areas by using (1) Tikhonov regularization (Tikhonov, 1963; Doherty, 2003; Fienen and others, 2009);

and (2) hybrid singular value decomposition (Tonkin and Doherty, 2005; Hunt and others, 2007), also referred to as SVD-Assist (SVDA) in Doherty (2010), at various times during the history-matching process. Additional information regarding the overview of the advantages of using these more sophisticated tools for parameter estimation are discussed by Hunt and others (2007); the tools were applied by using the guidelines given by Doherty and Hunt (2009).

Weighted Hydraulic-Head Observations

Hydraulic-head observations were weighted to reduce the influence of observations that were evaluated and determined to be less accurate and to increase the influence of observations determined to be more accurate. Accuracy of hydraulic-head observations was based on potential measurement error associated with the method of water-level measurement, determination of land-surface altitude and (or) spatial location of the well, effects of recent pumping, unknown screened interval or depth of the well, and other factors.

In the Ozark model area, there are hundreds of wells with a single groundwater-level measurement, a minority of wells that have periodic measurements spanning several months or years, and few wells with continuous data at daily (or less) intervals. Individual water-level measurements were evaluated to remove erroneous values from the observation data, including water levels above the land surface or below the depth of the well. Wells were eliminated or assigned low weight from the observation data if there was uncertainty pertaining to spatial location or well altitude, inconsistency between casing depth and well depth, and no lithologic data or well depth information, which would make water levels associated with the well almost useless in the history-matching process. The remaining wells in the observation dataset were then categorized as “poor,” “fair,” “good,” and “great.” For various metrics, individual values were assigned, and the product of all values for a single well was used to determine the category. A value ranging from zero to one was assigned for each of four metrics: (1) the relative certainty in land surface associated with the well; (2) the presence or absence of casing information; (3) the amount of lithologic data in the database and the hydrogeologic unit obtained by the intersection of the altitude of the bottom of the well and the framework data layers (Westerman and others, 2016a); and (4) the presence and magnitude of well depth, as shallow wells in the Ozark system may not reflect typical water levels in a thick hydrogeologic unit. The categories were assigned by the composite metric where values less than or equal to 0.3 were poor, less than or equal to 0.5 were fair, less than or equal to 0.7 were good, and greater than 0.7 were great. Initial weights for each category (poor, fair, and others) were assigned arbitrarily and adjusted during the PEST history-matching process to allow each category a part of the overall contribution to the objective function. The approximate part of each category of poor, fair, good, and great was 5, 10, 15, and 40 percent, respectively.

Over half of the observations (56 percent) occur in the lower Ozark aquifer, followed by the middle Ozark aquifer (19 percent), and the Springfield Plateau aquifer (14 percent), with the remaining spread throughout the Western Interior confining unit, upper Ozark aquifer, and the St. Francois aquifer. The observations used in the model are spread temporally from the early 1900s to 2013 with a rapid increase in the number of observations occurring after about 1953. An additional 5 percent of the objective function was composed of observations from continuous record wells (Missouri Department of Natural Resources, 2017). Water levels from the continuous records were averaged by month and included to evaluate the potential to capture simulated seasonal fluctuations in water levels. The remaining part of the objective function represented stream leakage observations.

Stream Leakage as Observations

Stream leakage, derived from streamflow measurements from digitized seepage-run studies (Knierim and others, 2015), was used as observations in the Ozark model through the River Observation (RVOB) Package (Harbaugh and Hill, 2009). Values of streamflow gain or loss computed by Knierim and others (2015) were summed to calculate a net gain or loss value for approximately 81 named streams (as opposed to stream-reach segments). As with hydraulic-head observations, stream leakage values were weighted to form a part (about 25 percent) of the overall objective function. Weighting of stream leakage normalizes the residuals to values that correspond more closely with those of hydraulic head because the residuals between the two data types vary as much as several orders of magnitude.

Base flow to a stream from the groundwater system can be approximated from the minimum 7-day, 2-year streamflow (7Q2) statistic (Imes and Emmett, 1994; Richards, 2010). This low-flow streamflow statistic was computed for 28 gaging stations that have a continuous record of streamflow for a minimum of 8 years. Because the 7Q2 statistic is based on many years of record, it represents more of the average cumulative base flow to the entire basin in relation to the precipitation received by that basin over the period of record. These values were used as calibration flow targets in the first stress period of the model when average recharge, no pumping, and steady-state conditions are simulated. These base-flow values were weighted to form a part of the overall objective function.

Model Evaluation

Optimal Parameter Estimates

The final parameter estimates of the model (table 2) are considered reasonable for the lithology and conditions found in the Ozark system. For aquifers and confining units, horizontal hydraulic conductivity estimates of

3.28×10^{-3} to 32.19 ft/d and 1.0×10^{-8} to 5.12×10^{-1} ft/d, respectively, are comparable to published estimates (Hays and others, 2016). Generally, values for hydraulic conductivity are within one to two orders of magnitude for a given hydrogeologic unit and represent estimates for large areas within the Ozark system (fig. 5). Specific yield and specific storage estimates were among the least sensitive parameters (discussed later in “Sensitivity and Identifiability”) and were specified as uniform values for most layers (table 2). Vertical hydraulic conductivity estimates range from 1.0×10^{-9} to 3.22 ft/d (fig. 5). Streambed conductance for each stream varied by model cell, according to streambed hydraulic conductivity, streambed thickness, stream length, and stream width. The final estimates of streambed conductance range from 8.0×10^{-3} to 2.05×10^8 ft²/d. Average simulated recharge estimates from 2000 to 2013, derived from EWB, range spatially from essentially zero to a maximum of 64.8 in/yr with a mean of 3.99 in/yr and a median of 3.91 in/yr. Some parameter estimates, such as those representing boundaries, particularly the CHD, were estimated beyond a range of perceived reasonable values and were reset to initial values. In the case of the CHD parameter, this may indicate a much wider range in prior head values than is currently thought to exist.

Model Fit and Model Error

Hydraulic-Head Observations and Errors

Simulated heads were generally in good agreement with observed hydraulic heads with 49 percent of simulated values within 60 ft of the observed value. Simulated heads were computed for 19,045 observed hydraulic-head measurements from 6,683 wells within the Ozark model area. Values of mean, minimum, maximum, root mean square error (RMSE), and absolute mean error were computed for each year from residuals (table 3). The RMSE, in feet, is determined by using the equation

$$\text{RMSE} = (h_o - h_s)^2 / n$$

where

- h_o is observed hydraulic head, in feet;
- h_s is simulated hydraulic head, in feet; and
- n is number of observations.

Values of RMSE (with greater than one observation per year) between simulated and observed hydraulic heads ranged from about 37 ft in 1929 to about 190 ft in 1916, whereas 37 annual RMSE values are less than 100 ft for the entire simulation period (table 3). The five greatest RMSE values occur from 1906 to 1969 and are attributed to the lack of accurate pumping data and the use of precipitation-adjusted recharge values for the time period. The RMSE for all observations in the model is 113 ft over a range in observed hydraulic head of 2,578 ft, where the range equals the difference between the highest and lowest observed hydraulic

Table 2. Final parameter estimates.

[All aquifer properties exclude Mississippi embayment values]

Parameter description	Parameter name	Value or range	Unit	Model layer
Hydraulic conductivity (horizontal)	hk1	4.71e-03 to 3.67e-01	feet/day	1
Hydraulic conductivity (horizontal)	hk2	2.83 to 6.48	feet/day	2
Hydraulic conductivity (horizontal)	hk3	1.31e-05 to 2.29e-02	feet/day	3
Hydraulic conductivity (horizontal)	hk4	4.33e-03 to 9.39e+00	feet/day	4
Hydraulic conductivity (horizontal)	hk5	3.28e-03 to 3.22e-01	feet/day	5
Hydraulic conductivity (horizontal)	hk6	0.30 to 32.19	feet/day	6
Hydraulic conductivity (horizontal)	hk7	1.00e-08 to 5.12e-01	feet/day	7
Hydraulic conductivity (horizontal)	hk8	10.52 to 12.53	feet/day	8
Hydraulic conductivity (horizontal)	hk9	10.52 to 12.53	feet/day	9
Hydraulic conductivity (vertical)	vk1	4.71e-04 to 3.67e-02	feet/day	1
Hydraulic conductivity (vertical)	vk2	0.28 to 0.65	feet/day	2
Hydraulic conductivity (vertical)	vk3	1.31e-06 to 2.29e-03	feet/day	3
Hydraulic conductivity (vertical)	vk4	4.33e-04 to 9.39e-01	feet/day	4
Hydraulic conductivity (vertical)	vk5	3.28e-04 to 3.22e-02	feet/day	5
Hydraulic conductivity (vertical)	vk6	0.03 to 3.22	feet/day	6
Hydraulic conductivity (vertical)	vk7	1.00e-09 to 5.12e-02	feet/day	7
Hydraulic conductivity (vertical)	vk8	1.05 to 1.25	feet/day	8
Hydraulic conductivity (vertical)	vk9	1.05 to 1.25	feet/day	9
Specific yield	sy1	0.02	dimensionless	1
Specific yield	sy2	1.00e-02	dimensionless	2
Specific yield	sy3	1.00e-02	dimensionless	3
Specific yield	sy4	3.00e-04 to 3.00e-03	dimensionless	4
Specific yield	sy5	3.00e-04	dimensionless	5
Specific yield	sy6	2.99e-03 to 8.97e-03	dimensionless	6
Specific storage	ss1	1.00e-05	1/day	1
Specific storage	ss2	1.00e-05	1/day	2
Specific storage	ss3	1.00e-04	1/day	3
Specific storage	ss4	5.00e-07	1/day	4
Specific storage	ss5	5.00e-07	1/day	5
Specific storage	ss6	3.84e-07 to 5.01e-06	1/day	6
Specific storage	ss7	5.00e-07	1/day	7
Specific storage	ss8	3.00e-07	1/day	8
Specific storage	ss9	3.00e-07	1/day	9
Recharge	rch	0.00e+00 to 6.48e+01	inch/year	multiple
Temporal recharge multipliers	tsrch1	0.94	dimensionless	multiple
Temporal recharge multipliers	tsrch2	0.92	dimensionless	multiple
Temporal recharge multipliers	tsrch3	0.89	dimensionless	multiple
Temporal recharge multipliers	tsrch4	0.94	dimensionless	multiple
Temporal recharge multipliers	tsrch5	0.81	dimensionless	multiple
Temporal recharge multipliers	tsrch6	0.91	dimensionless	multiple
Temporal recharge multipliers	tsrch7	1.03	dimensionless	multiple
Temporal recharge multipliers	tsrch8	0.93	dimensionless	multiple

Table 2. Final parameter estimates.—Continued

[All aquifer properties exclude Mississippi embayment values]

Parameter description	Parameter name	Value or range	Unit	Model layer
Temporal recharge multipliers	tsrch9	0.94	dimensionless	multiple
Temporal recharge multipliers	tsrch10	0.78	dimensionless	multiple
Temporal recharge multipliers	tsrch11	0.92	dimensionless	multiple
Temporal recharge multipliers	tsrch12	1.27	dimensionless	multiple
Temporal recharge multipliers	tsrch13	1.01	dimensionless	multiple
Temporal recharge multipliers	tsrch14	1.00	dimensionless	multiple
Temporal recharge multipliers	tsrch15	0.68	dimensionless	multiple
Temporal recharge multipliers	tsrch16	0.97	dimensionless	multiple
Temporal recharge multipliers	tsrch17	0.92	dimensionless	multiple
Temporal recharge multipliers	tsrch18	0.95	dimensionless	multiple
Temporal recharge multipliers	tsrch19	0.62	dimensionless	multiple
Temporal recharge multipliers	tsrch20	0.97	dimensionless	multiple
Temporal recharge multipliers	tsrch21	1.18	dimensionless	multiple
Temporal recharge multipliers	tsrch22	1.00	dimensionless	multiple
Temporal recharge multipliers	tsrch23	1.07	dimensionless	multiple
Temporal recharge multipliers	tsrch24	1.26	dimensionless	multiple
Temporal recharge multipliers	tsrch25	0.99	dimensionless	multiple
Temporal recharge multipliers	tsrch26	0.98	dimensionless	multiple
Temporal recharge multipliers	tsrch27	0.91	dimensionless	multiple
Temporal recharge multipliers	tsrch28	0.76	dimensionless	multiple
Streambed conductance	huc103	22.40 to 2,513,500	feet ² /day	multiple
Streambed conductance	huc105	1.36 to 654,900	feet ² /day	multiple
Streambed conductance	huc106	3,650.00 to 29,215,000	feet ² /day	multiple
Streambed conductance	huc107	4.65 to 79,020	feet ² /day	multiple
Streambed conductance	huc108	7,160.00 to 57,700,000	feet ² /day	multiple
Streambed conductance	huc114	1.41 to 59,568	feet ² /day	multiple
Streambed conductance	huc116	0.01 to 16,780.00	feet ² /day	multiple
Streambed conductance	huc117	1,420.00 to 204,850,000	feet ² /day	multiple
Streambed conductance	huc118	5.15 to 195,300	feet ² /day	multiple
Streambed conductance	huc119	7.73 to 194,640	feet ² /day	multiple
Streambed conductance	huc12	7.16 to 553,400	feet ² /day	multiple
Streambed conductance	huc120	2,015.00 to 14,730,000	feet ² /day	multiple
Streambed conductance	huc122	559,900	feet ² /day	multiple
Streambed conductance	huc130	6.44 to 315,300	feet ² /day	multiple
Streambed conductance	huc131	340.60 to 1,714.00	feet ² /day	multiple
Streambed conductance	huc132	4.00 to 39,330.00	feet ² /day	multiple
Streambed conductance	huc134	1,640.00 to 65,550,000	feet ² /day	multiple
Streambed conductance	huc135	1.40 to 212,700	feet ² /day	multiple
Streambed conductance	huc136	3.01 to 1,426.00	feet ² /day	multiple
Streambed conductance	huc138	15.98 to 65,790.00	feet ² /day	multiple
Streambed conductance	huc140	0.57 to 64,920.00	feet ² /day	multiple
Streambed conductance	huc141	0.81 to 47,650.00	feet ² /day	multiple

Table 2. Final parameter estimates.—Continued

[All aquifer properties exclude Mississippi embayment values]

Parameter description	Parameter name	Value or range	Unit	Model layer
Streambed conductance	huc146	0.44 to 63,030.00	feet ² /day	multiple
Streambed conductance	huc147	23.90 to 44,560.00	feet ² /day	multiple
Streambed conductance	huc149	3,750.00 to 23,855,000	feet ² /day	multiple
Streambed conductance	huc150	44.45 to 12,140.00	feet ² /day	multiple
Streambed conductance	huc151	4.97 to 52,790.00	feet ² /day	multiple
Streambed conductance	huc153	117.40 to 11,380.00	feet ² /day	multiple
Streambed conductance	huc154	15.00 to 94,400,000	feet ² /day	multiple
Streambed conductance	huc170	12.00 to 204,050	feet ² /day	multiple
Streambed conductance	huc176	5.76 to 141,000	feet ² /day	multiple
Streambed conductance	huc177	0.11 to 22,250.00	feet ² /day	multiple
Streambed conductance	huc178	2.61 to 52,710.00	feet ² /day	multiple
Streambed conductance	huc179	5.80 to 31,380.00	feet ² /day	multiple
Streambed conductance	huc180	40.78 to 15,140.00	feet ² /day	multiple
Streambed conductance	huc182	30.55 to 34,180.00	feet ² /day	multiple
Streambed conductance	huc183	14.35 to 306,850	feet ² /day	multiple
Streambed conductance	huc184	1.05 to 465,250	feet ² /day	multiple
Streambed conductance	huc187	6.69 to 51,160.00	feet ² /day	multiple
Streambed conductance	huc188	3,690.00 to 44,355,000	feet ² /day	multiple
Streambed conductance	huc208	19.80 to 1,098,000	feet ² /day	multiple
Streambed conductance	huc214	1.80 to 114,500	feet ² /day	multiple
Streambed conductance	huc218	0.008 to 37,500.00	feet ² /day	multiple
Streambed conductance	huc241	55.00 to 57,450,000	feet ² /day	multiple
Streambed conductance	huc242	10.85 to 269,300	feet ² /day	multiple
Streambed conductance	huc243	14.25 to 2,489,500	feet ² /day	multiple
Streambed conductance	huc251	1.69 to 2,916.00	feet ² /day	multiple
Streambed conductance	huc77	1.59 to 76,580.00	feet ² /day	multiple
Streambed conductance	huc78	10.29 to 156,400	feet ² /day	multiple
Streambed conductance	huc79	0.10 to 130,600	feet ² /day	multiple
Streambed conductance	huc80	1.86 to 76,850.00	feet ² /day	multiple
Streambed conductance	huc81	8.82 to 722,200	feet ² /day	multiple
Streambed conductance	huc82	5.30 to 448,800	feet ² /day	multiple
Streambed conductance	huc83	1.91 to 67,740.00	feet ² /day	multiple
Streambed conductance	huc84	11.45 to 879,500	feet ² /day	multiple
Streambed conductance	huc90	17.06 to 131,000	feet ² /day	multiple
Streambed conductance	huc98	6.89 to 1,122,000	feet ² /day	multiple
Streambed conductance	huc99	5.01 to 1,100,000	feet ² /day	multiple
General head multiplier	ghb-1	1.00	dimensionless	multiple
Constant head multiplier	chd-1	1.00	dimensionless	multiple
Horizontal flow multiplier	hfb-1	1.00	dimensionless	multiple
Pumping multiplier	wel-1	1.00	dimensionless	multiple

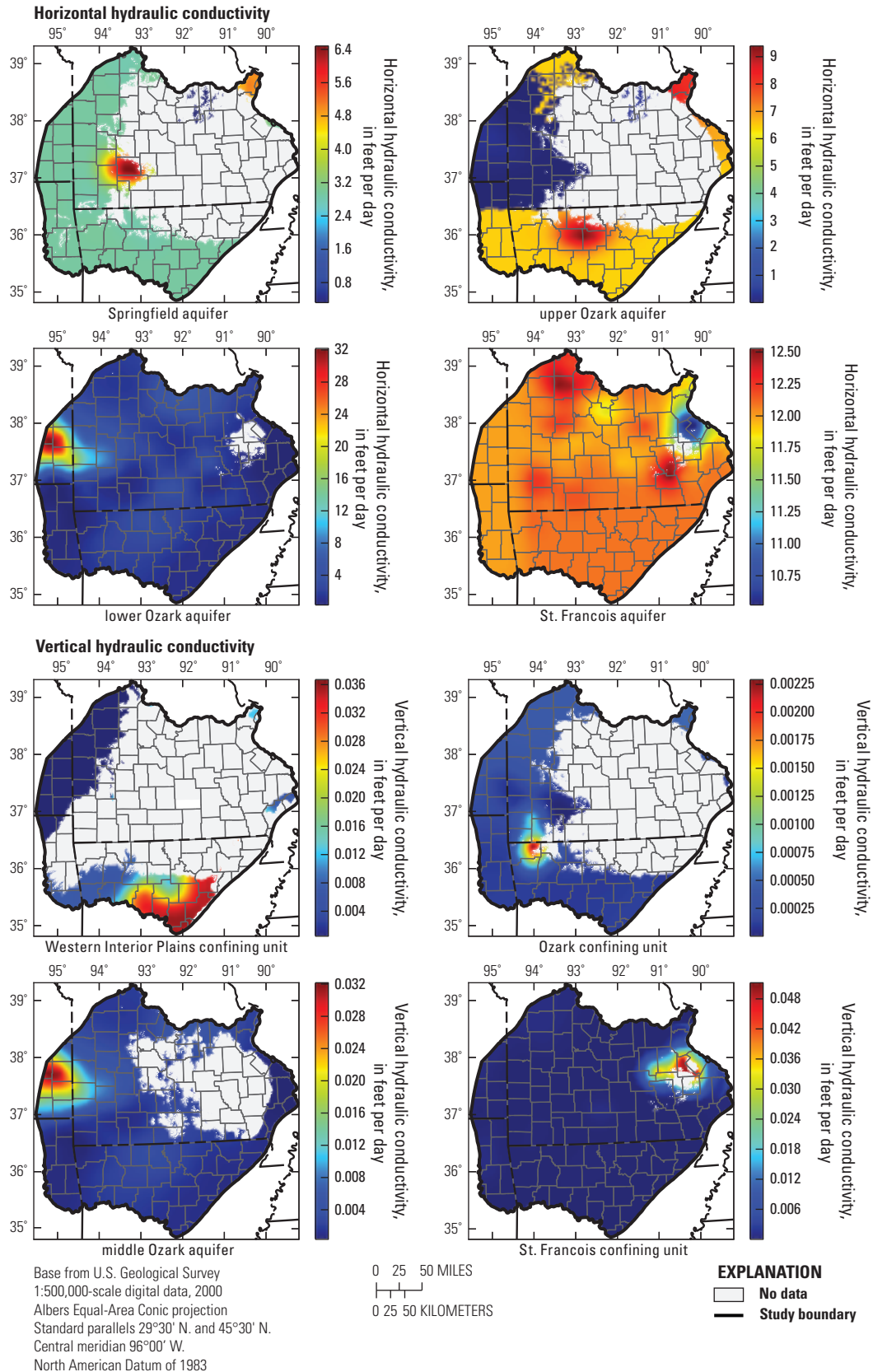


Figure 5. Horizontal and vertical hydraulic conductivity of model layers that utilize pilot points. The contrast in values of layer 4 in the west-central study area indicates absence of layer; properties are inherited from adjacent units.

Table 3. Summary of hydraulic-head residual statistics for model calibration.

[RSME, root mean square error; --, no value]

Year	Mean residual (feet)	Minimum residual (feet)	Maximum residual (feet)	Root mean square error (RMSE) (feet)	Mean absolute error (feet)	Number of observations	Range (feet)	Ratio of RMSE to range
1900	14	14	14	--	14	1	0	--
1905	-104	-229	-18	138	104	3	580	0.24
1906	-197	-197	-197	--	197	1	0	--
1907	-32	-107	43	82	75	2	7	11.72
1908	-52	-52	-52	--	52	1	0	--
1910	-99	-99	-99	--	99	1	0	--
1911	-143	-143	-143	--	143	1	0	--
1912	-27	-95	18	56	39	3	175	0.32
1913	-137	-137	-137	--	137	1	0	--
1914	-102	-307	23	178	118	3	152	1.17
1915	-62	-189	26	90	70	6	709	0.13
1916	-183	-245	-120	190	183	5	445	0.43
1917	-102	-126	-58	106	102	3	59	1.8
1918	-36	-65	-8	46	36	2	89	0.52
1921	-145	-145	-145	--	145	1	0	--
1922	-12	-12	-12	--	12	1	0	--
1923	-24	-109	25	65	49	3	321	0.2
1924	-65	-95	-25	71	65	3	211	0.34
1925	-19	-96	20	58	45	3	488	0.12
1926	-79	-241	51	126	96	11	915	0.14
1927	-109	-170	-49	125	109	2	164	0.76
1928	32	-11	67	45	39	3	860	0.05
1929	-30	-65	8	37	32	6	745	0.05
1930	-31	-208	73	92	62	6	447	0.21
1931	-42	-159	122	97	77	9	908	0.11
1932	-15	-58	46	42	37	8	829	0.05
1933	-14	-145	160	65	46	19	886	0.07
1934	-56	-185	88	85	68	34	931	0.09
1935	-40	-171	108	78	64	35	946	0.08
1936	-26	-210	101	67	53	167	1,024	0.07
1937	-11	-169	142	62	50	71	1,214	0.05
1938	-21	-271	195	98	75	89	1,235	0.08
1939	-20	-243	142	76	60	92	1,021	0.07
1940	-22	-250	180	74	55	112	889	0.08
1941	-15	-282	171	76	57	101	1,024	0.07
1942	-57	-385	102	116	85	121	1,197	0.1

Table 3. Summary of hydraulic-head residual statistics for model calibration.—Continued

[RSME, root mean square error; --, no value]

Year	Mean residual (feet)	Minimum residual (feet)	Maximum residual (feet)	Root mean square error (RMSE) (feet)	Mean absolute error (feet)	Number of observations	Range (feet)	Ratio of RMSE to range
1943	-65	-346	123	114	88	41	822	0.14
1944	-54	-383	161	134	102	27	846	0.16
1945	-35	-397	157	105	68	26	989	0.11
1946	-24	-281	167	94	69	75	1,053	0.09
1947	-22	-252	123	83	60	75	1,030	0.08
1948	-68	-331	89	112	84	66	956	0.12
1949	-35	-209	337	111	80	46	1,948	0.06
1950	-10	-268	650	152	114	58	1,478	0.1
1951	-10	-209	164	108	85	64	1,327	0.08
1952	-90	-334	134	131	105	46	1,071	0.12
1953	-50	-277	467	148	109	60	1,596	0.09
1954	-80	-288	185	121	99	112	1,222	0.1
1955	-53	-408	207	112	84	166	1,195	0.09
1956	-70	-366	155	126	90	141	1,159	0.11
1957	-91	-353	198	149	109	163	1,065	0.14
1958	-61	-414	159	119	88	122	1,166	0.1
1959	-56	-317	360	119	87	135	1,096	0.11
1960	-32	-324	427	116	85	317	1,193	0.1
1961	-16	-390	467	130	97	270	1,509	0.09
1962	17	-244	473	146	105	381	1,342	0.11
1963	-18	-233	443	119	90	261	1,365	0.09
1964	5	-292	254	82	62	451	1,236	0.07
1965	-6	-254	577	84	58	400	1,633	0.05
1966	-30	-893	175	105	70	252	1,149	0.09
1967	-35	-254	263	94	72	244	1,164	0.08
1968	0	-611	800	156	95	213	1,717	0.09
1969	-68	-598	211	156	105	130	1,157	0.13
1970	-52	-363	149	107	79	151	1,119	0.1
1971	-62	-463	135	122	91	118	1,046	0.12
1972	-78	-407	106	132	102	128	1,039	0.13
1973	-57	-385	139	112	86	230	1,103	0.1
1974	-88	-440	146	140	106	203	1,037	0.14
1975	-90	-414	423	130	101	197	1,528	0.09
1976	-49	-379	107	98	74	184	1,100	0.09
1977	-80	-244	269	116	93	221	1,178	0.1
1978	-48	-416	164	112	88	285	1,119	0.1

Table 3. Summary of hydraulic-head residual statistics for model calibration.—Continued

[RSME, root mean square error; --, no value]

Year	Mean residual (feet)	Minimum residual (feet)	Maximum residual (feet)	Root mean square error (RMSE) (feet)	Mean absolute error (feet)	Number of observations	Range (feet)	Ratio of RMSE to range
1979	-112	-400	142	138	116	165	1,034	0.13
1980	-99	-428	549	147	115	165	1,441	0.1
1981	-110	-427	85	138	115	482	995	0.14
1982	-83	-380	138	120	96	526	1,039	0.12
1983	-77	-303	138	122	94	146	827	0.15
1984	-112	-291	47	138	115	146	921	0.15
1985	-118	-312	55	147	124	166	995	0.15
1986	-112	-281	126	145	122	173	980	0.15
1987	-65	-496	370	126	96	276	1,845	0.07
1988	-51	-334	469	122	93	156	1,690	0.07
1989	-36	-621	456	122	83	248	1,570	0.08
1990	-37	-777	733	135	90	303	1,853	0.07
1991	-18	-347	719	113	77	303	1,720	0.07
1992	-14	-277	354	107	82	411	1,503	0.07
1993	12	-442	346	105	77	371	1,550	0.07
1994	-29	-223	246	94	66	77	1,006	0.09
1995	-43	-424	215	88	67	652	1,057	0.08
1996	-21	-349	217	100	72	125	1,133	0.09
1997	-38	-352	191	105	74	58	1,057	0.1
1998	-5	-278	213	81	60	346	1,049	0.08
1999	-36	-222	238	86	73	189	665	0.13
2000	-33	-359	199	92	70	658	926	0.1
2001	-29	-860	347	89	63	628	1,795	0.05
2002	-34	-487	169	79	66	738	1,169	0.07
2003	-29	-330	151	76	66	765	1,130	0.07
2004	-46	-860	343	124	83	352	1,616	0.08
2005	-18	-445	151	91	66	298	1,041	0.09
2006	-43	-592	210	120	82	623	1,074	0.11
2007	-48	-865	250	125	88	452	1,547	0.08
2008	-68	-483	186	123	93	302	1,105	0.11
2009	-54	-499	185	114	85	440	1,089	0.1
2010	-69	-935	314	140	98	507	1,562	0.09
2011	-59	-499	181	119	90	396	1,111	0.11
2012	-62	-483	167	125	95	349	1,109	0.11
2013	-79	-634	86	145	106	64	846	0.17
all	-44	-935	800	113	83	19,045	2,578	0.04

head. The model results were also evaluated through the calculation of the mean residual for the hydraulic heads. The mean of residuals indicates model bias depending on the magnitude and direction of the mean away from zero. A mean close to zero because of a balance between positive and negative residuals indicates less model bias. A positive mean indicates the model tends to underpredict (simulated hydraulic heads less than observed) water-level altitude, and a negative mean indicates overprediction (simulated hydraulic heads greater than observed) of water levels. The mean residual approached zero with an absolute value less than 20 ft during 20 of the 107 years for which residuals were calculated. Out of 19,045 observations, 6,314 residuals were greater than or equal to zero (underprediction) and 12,731 residuals were less than zero (overprediction) (fig. 6), resulting in a mean residual of -44 ft. The maximum and minimum residuals were 800 and -935 ft, occurring in 1968 and 2010, respectively. Some of the largest positive residuals were located in the southern part of the model area within the Western Interior Plains confining unit. These observations were within the “poor” category of head observations, which indicates uncertainty in well construction information or a relatively shallow well in the comparably thick model layer. The largest negative residuals were located horizontally near the southern and eastern interior extent of model layer 2 (Springfield Plateau aquifer) and vertically in the middle and lower Ozark aquifer. These observations were also within the “poor” category of head observations.

Graphical analyses of the residuals facilitate assessment of model bias or error and of model fit to the observation data. These analyses include plots of the observed and simulated values and the spatial and temporal distribution of the hydraulic-head residuals. The model fit generally is similar over the entire range of available hydraulic-head values, and the calibration has, in general, an acceptable distribution of residuals above and below the 1:1 line (fig. 7).

Additional assessments of model error are accomplished through analysis of the spatial distribution of residuals. Negative residuals indicate simulated hydraulic heads that are higher than observed (overpredicted), whereas positive residuals indicate simulated hydraulic heads that are lower than observed (underpredicted) (fig. 8). In general, there appears to be a bias toward overprediction of water levels in the western part of the model area in the confined part of the Ozark aquifer. Although many realizations of model simulations were explored during history matching, none seemed to effectively eliminate this bias. Some current potential explanations for this bias lie in the uncertainty of water-use estimates and the cell size of the model grid. As noted in the “Groundwater Pumpage” section, water use within Ottawa County, Oklahoma, was increased, which decreased but did not eliminate the bias. Similar increases in water use may be expected in other parts of the model domain. Additionally, the cell size used in the model grid may affect the amount of water-level decline and the simulated head at a given observation location. Because all pumping within a model cell is represented at the center of the cell, the largest

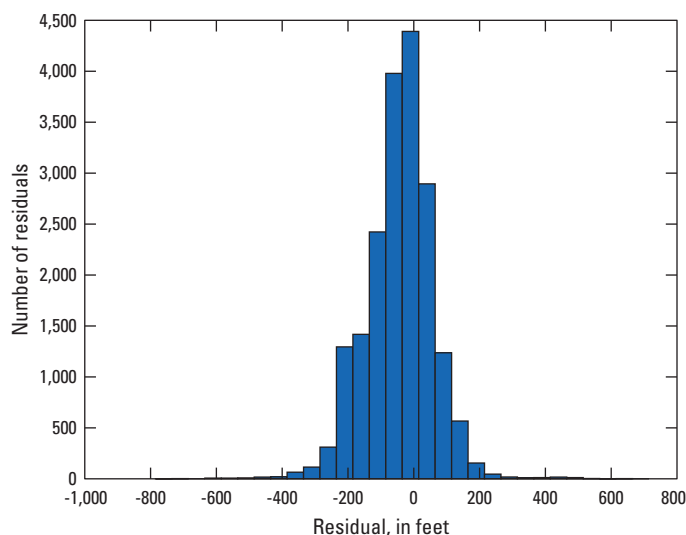


Figure 6. Unweighted hydraulic-head residuals.

water-level decline will be expected at that location. If a water-level observation is located near the edge of the model cell, it is possible that the simulated head at that location could vary substantially from that of the cell center.

Streamflow Observations and Errors

Simulated stream leakage and the 7Q2 statistic values generally are overpredicted compared to estimated leakage (fig. 9), meaning that the model overestimates discharge from the aquifer system to streams. Stream leakage is underpredicted (less discharge from aquifer to stream or possibly losing stream) for 36 observations and overpredicted for 97 observations in the model. Streamflow data, upon which stream leakage is computed, were collected by measuring streamflow at points along a stream as well as at tributaries and springs contributing water to that stream. Streamflow measurements inherently have some amount of error, which can propagate into the estimate of stream leakage, especially at small flows that included many of the tributary measurements and estimates from Knierim and others (2015).

Simulated and Observed Hydrographs

Simulated and observed water levels in 10 selected wells completed in the Springfield Plateau aquifer, the Ozark aquifer, and the St. Francois aquifer were used to examine the temporal trends of the model (fig. 10). The hydrographs show similar trends in water-level altitude for most locations. Some hydrographs showing a poorer fit to observed conditions overpredict heads throughout the period of measurement. Many of these differences are likely because of the placement and timing of pumping wells in the model, which are dependent on the accuracy of pumping data, as well as uncertainty in hydraulic property values, model boundary conditions, and recharge.

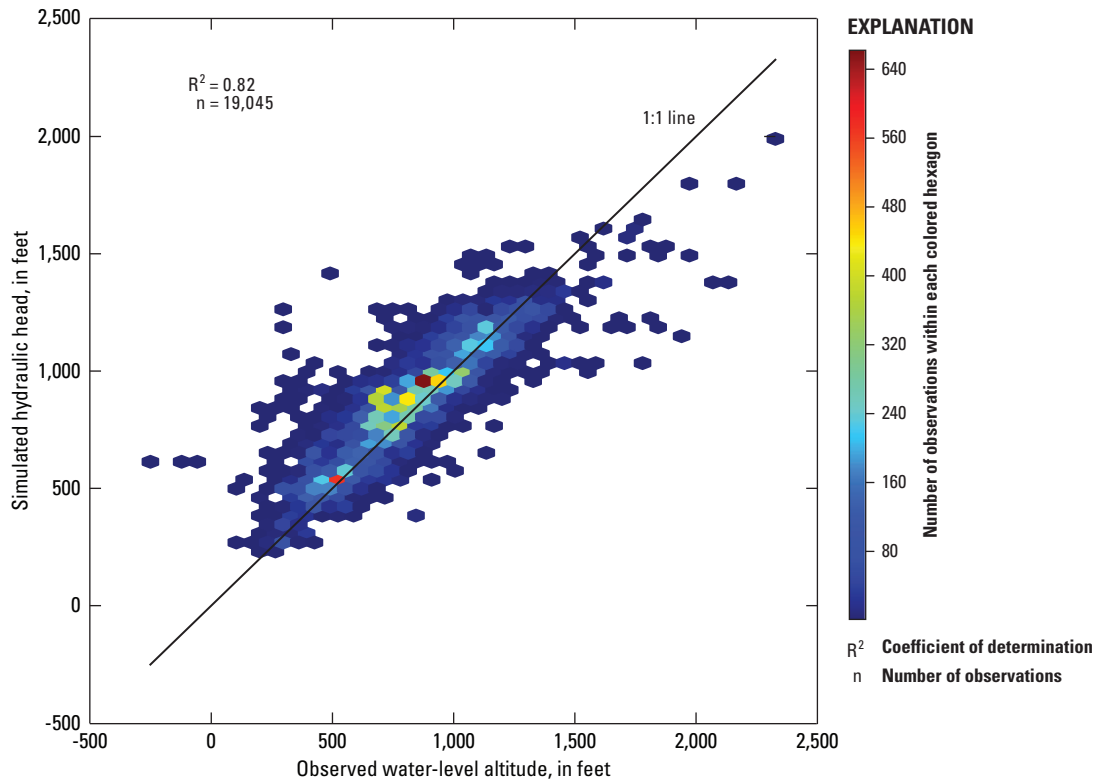


Figure 7. Unweighted simulated hydraulic-head values plotted against observed.

Simulated and Observed Potentiometric Surfaces

The simulated potentiometric surface of the Ozark aquifer (layer 6) for 2014 generally agrees with the observed potentiometric surface representing the winter of 2014–15 (fig. 11; Nottmeier, 2015). The potentiometric surface from Nottmeier (2015) was constructed by using water-level measurements from 178 wells in the model area for the Ozark aquifer. The potentiometric surface indicates a relief in water-level altitude of over 1,000 ft from the highest to the lowest measured water level in the Ozark aquifer. Potentiometric-surface contours for the winter of 2014, overlain on simulated hydraulic heads, give a reasonable qualitative match for the Ozark system, thus showing the model represents the general topography and flow directions of groundwater in the Ozark aquifer.

Sensitivity and Identifiability

The sensitivity of hydraulic heads and stream leakage to various model parameters is contained within the Jacobian matrix calculated by using PEST++ (Welter and others, 2015). The Jacobian matrix relates sensitivity values of each observation to each parameter and is used to estimate changes

in parameter values during the history-matching process. Sensitivity values for defined groups of parameters can be summed to provide a simple view of model inputs that could provide control over history matching (fig. 12); however, sensitivities calculated in this manner ignore parameter correlation, which indicates changes in one parameter can be offset by changes in another parameter where the result is a set of nonunique parameter values (Hill and Østerby, 2003). Parameter identifiability (Doherty and Hunt, 2009) indicates how well a parameter may be constrained by the observations used in history matching, or in other words, how well the parameter may be uniquely estimated based on available observations. Identifiability of the top 30 parameters differs from parameter group sensitivities in that boundaries such as CHD, pumping multipliers, and temporal recharge multipliers occur as more identifiable parameters (fig. 13), though vertical hydraulic conductivity of layers 3 and 5 (vk3 and vk5) tends to occur as more sensitive (fig. 12). One parameter with high identifiability, 119vk3, is a pilot point that represents the vertical hydraulic conductivity of layer 3 near the extreme southern boundary of the model area. This parameter may be affected by the assumption of a no-flow boundary condition along the southern boundary of the model, whereby groundwater would be forced upward through layer 3 to surficial discharge points.

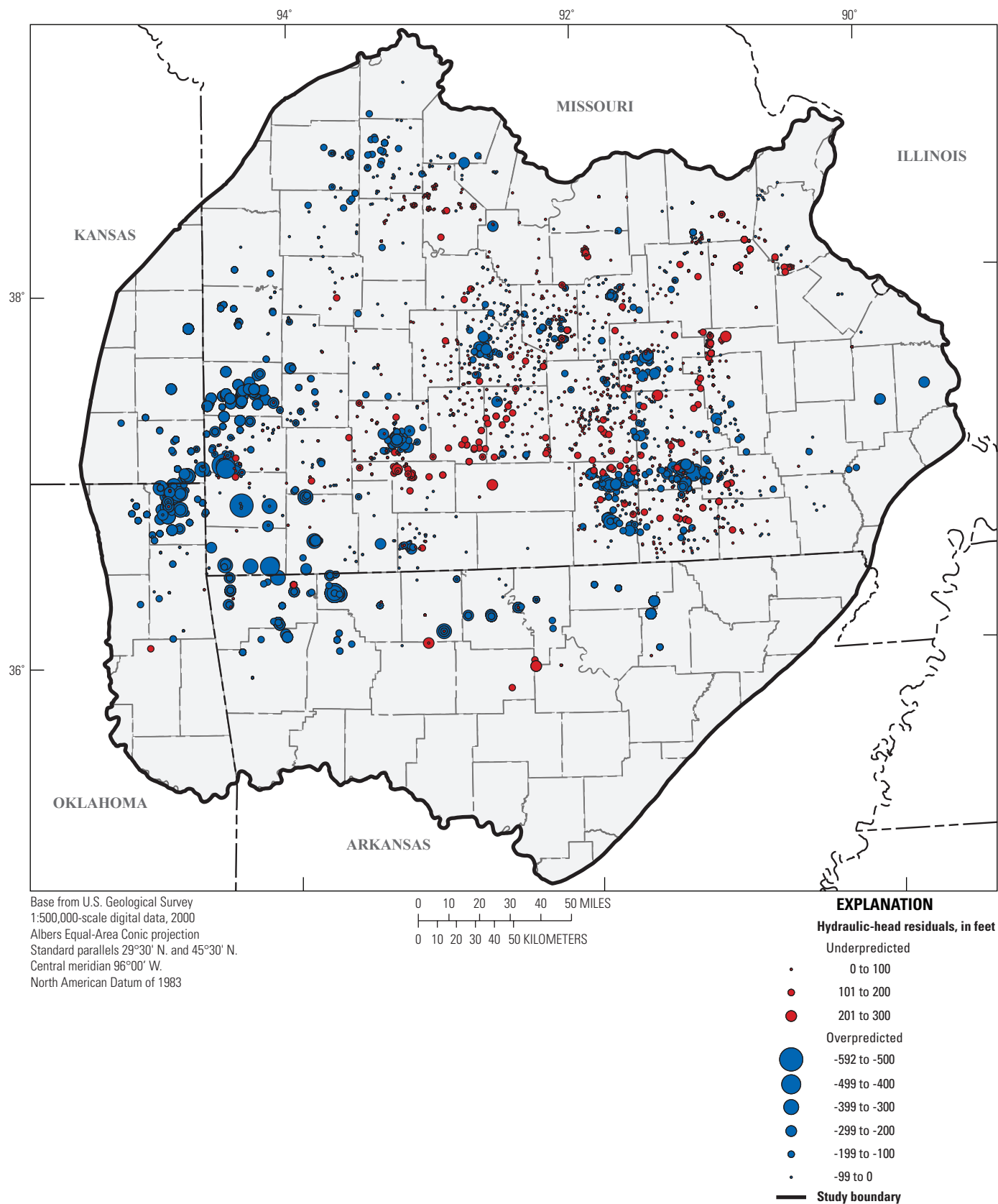


Figure 8. Spatial distribution of hydraulic-head residuals for the lower Ozark aquifer excluding observations categorized as “poor.”

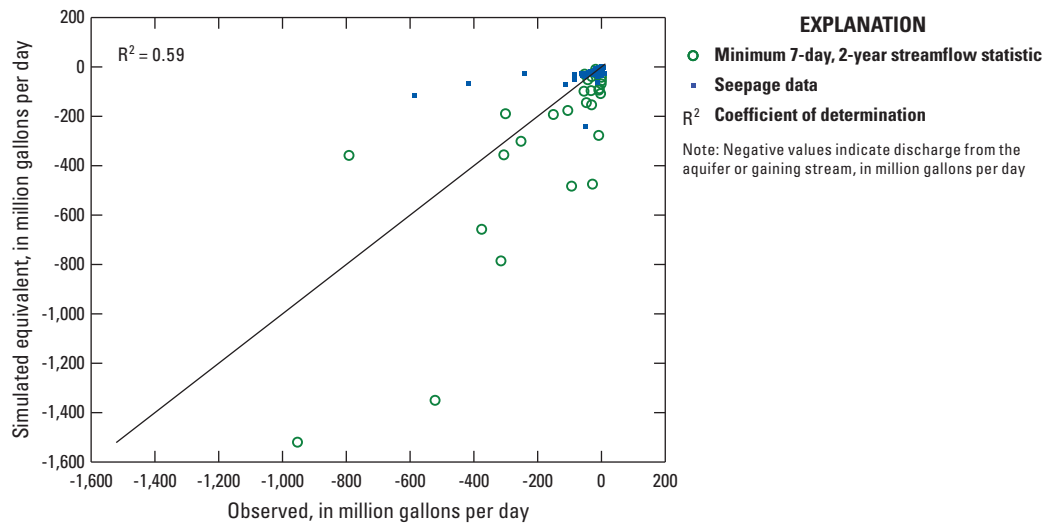


Figure 9. Simulated stream leakage plotted against observed stream leakage.

Groundwater-Flow Budget

The groundwater-flow budget indicates changes in flow into (inflows) and out of (outflows) the model area from the predevelopment period (pre-1900) to 2015 (fig. 14). Negative rates indicate outflows from the groundwater system and positive rates indicate inflows to the groundwater system. The main source of water to the Ozark system is precipitation, and the amount not routed to evapotranspiration, plant uptake, or runoff contributes recharge to the aquifers (Hays and others, 2016). Recharge, the largest inflow component, ranges seasonally from about 1,900 Mgal/d in spring/summer to 27,500 Mgal/d in fall/winter with a mean of 12,000 Mgal/d. Smaller inflows occur through losing-stream reaches and surface-water and groundwater inflow (Hays and others, 2016), although these values are small enough that they do not result in a net inflow to the Ozark system. The dominant outflow component from the Ozark system occurs as discharge to gaining streams and fluctuates seasonally between 7,500 and 17,500 Mgal/d with a mean outflow of 11,500 Mgal/d. Much of the remaining balance between recharge inflows and stream outflows is made up by water moving into or out of storage in the system. Groundwater pumping increases throughout the simulation period with a maximum rate of about 600 Mgal/d. Outflows to constant heads represent the groundwater interaction along the western extent of the model area (fig. 4). The constant-head boundary follows approximately 209 mi of the active model extent with a mean net outflow of 138 Mgal/d. This equates to about 0.66 million gallons per day per mile (Mgal/d/mi), or 1 cubic foot per second (ft³/s) per mile. Specified heads representing the boundary with the Mississippi embayment aquifer system indicate an average outflow of about 125 Mgal/d, though this value accounts for flow from both the Ozark system and groundwater flow within the layers representing the MERAS units (fig. 14).

Limitation of Analysis

An understanding of model limitations is essential to effectively use flow and hydraulic-head simulation results. The accuracy of a groundwater model is limited by simplification of complexities within the flow system (conceptual model), space and time discretization effects, and assumptions made in the formulation of the governing flow equations. Model accuracy is affected by cell size, number of layers, accuracy of boundary conditions, accuracy and availability of hydraulic property data, accuracy of groundwater pumping and areal recharge estimates, historical data available for calibration, parameter sensitivity, and the interpolations and extrapolations that are inherent in using data in a model. Although a model might be calibrated, the calibration parameter values are not unique in yielding acceptable distributions of hydraulic head. Structural error also exists through the assumption of boundaries, such as no-flow areas or the exclusion of faults, which cannot be quantified individually through parameter sensitivity or identifiability.

In the Ozark system model, flow in and out of the overlying alluvial material and the underlying or adjacent groundwater systems presumably represents a relatively small percentage of the overall water budget. Alluvial deposits that occur along the Missouri, Mississippi, Arkansas, and other large rivers were not explicitly simulated in the model. Pumpage and observations in alluvial deposits were largely ignored. Groundwater flow from underlying or adjacent systems is not well defined, though the contribution from such systems is considered negligible compared to the overall flow within the Ozark system. For example, flow in the alluvial material in the adjacent Mississippi embayment is marginally represented through boundary conditions and average aquifer properties. The assumption of a no-flow boundary near the freshwater-saline water interface (at the northwestern boundary of the Ozark system) and constant density of water may not be entirely

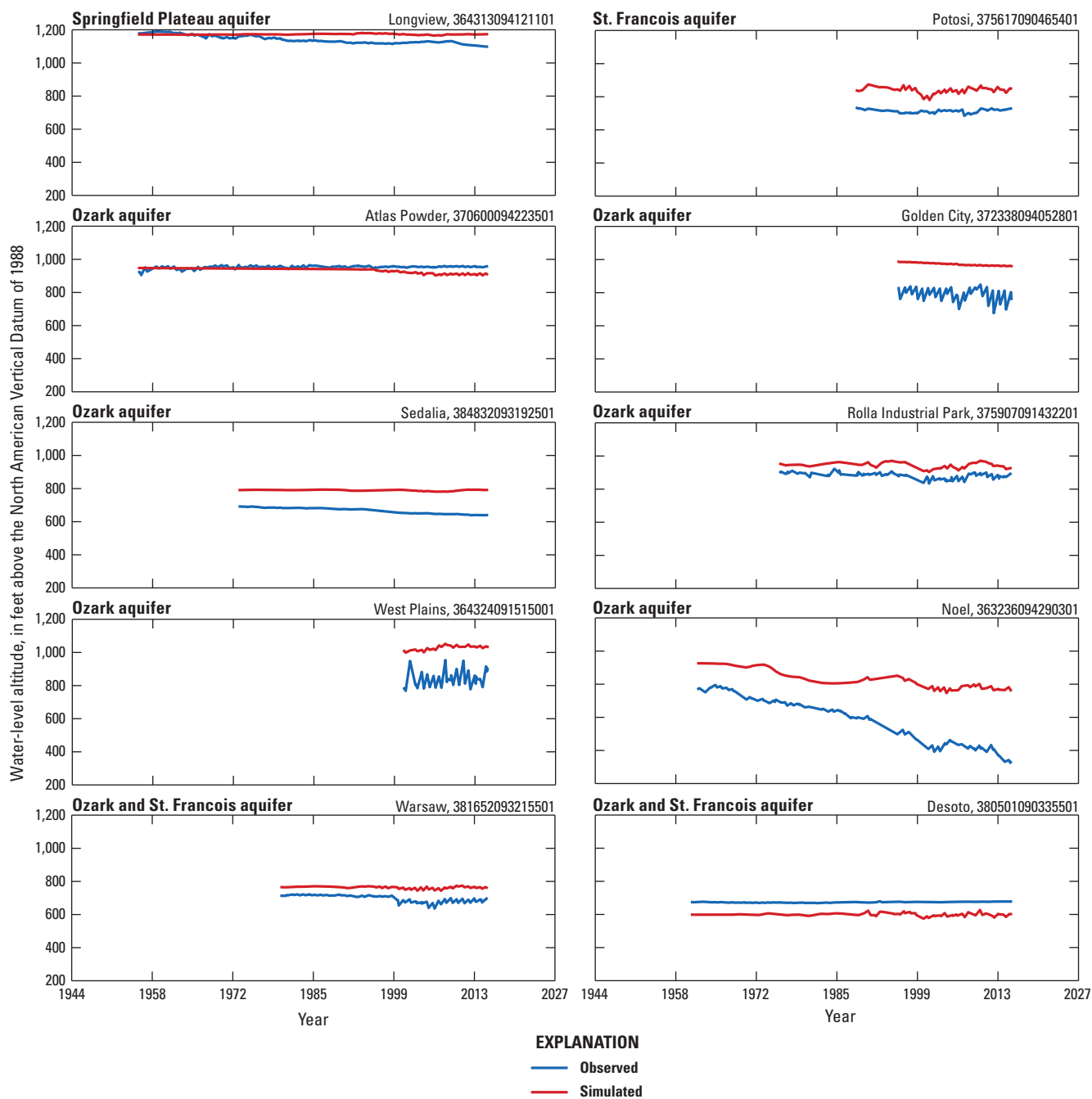


Figure 10. Simulated and observed water levels in selected wells. Name and number at top and right of each graph are the U.S. Geological Survey well name and identifier. Well locations are shown in figure 1.

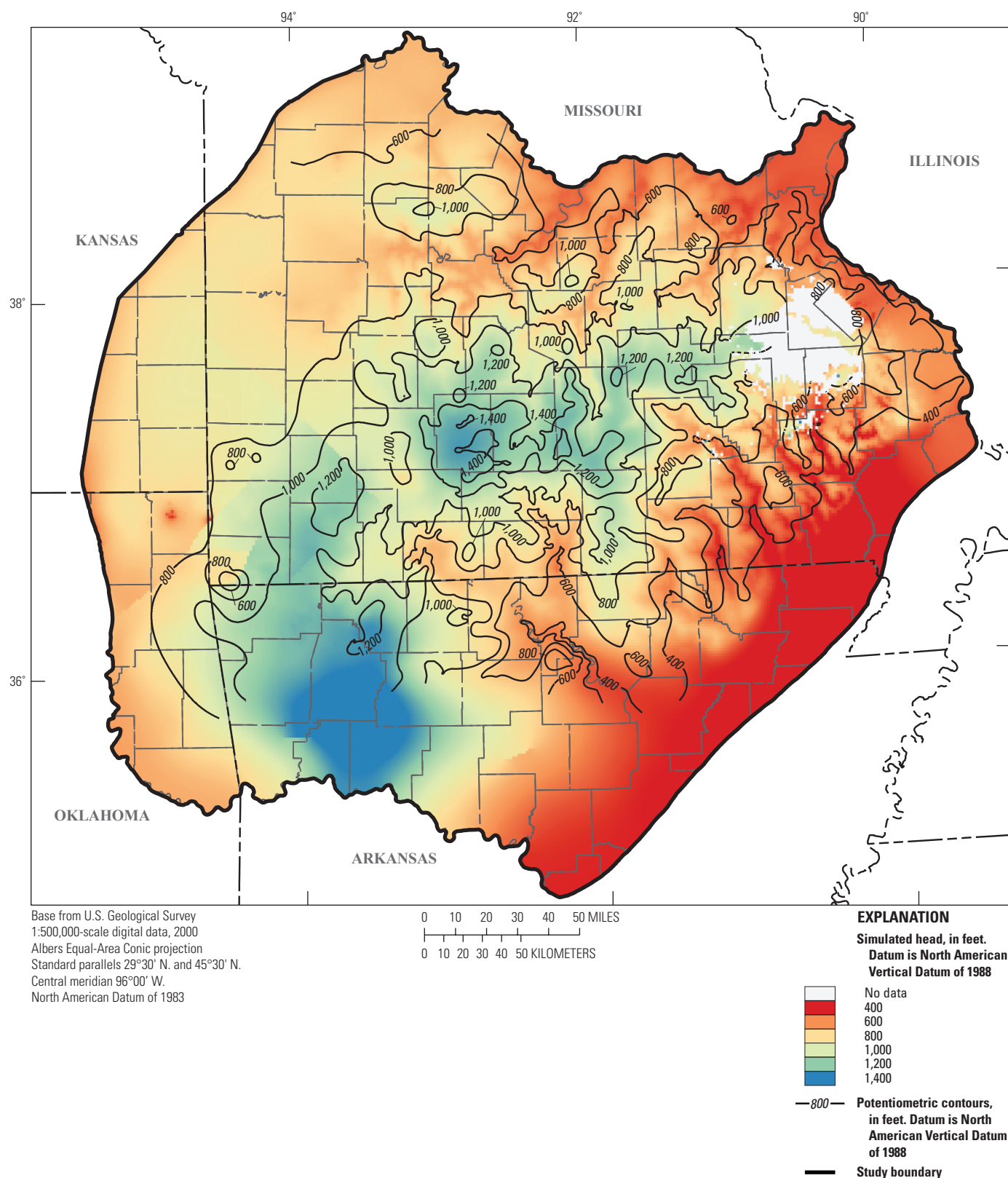


Figure 11. Potentiometric surface and simulated water levels for the Ozark aquifer, winter of 2014–15. Modified from Nottmeier (2015).

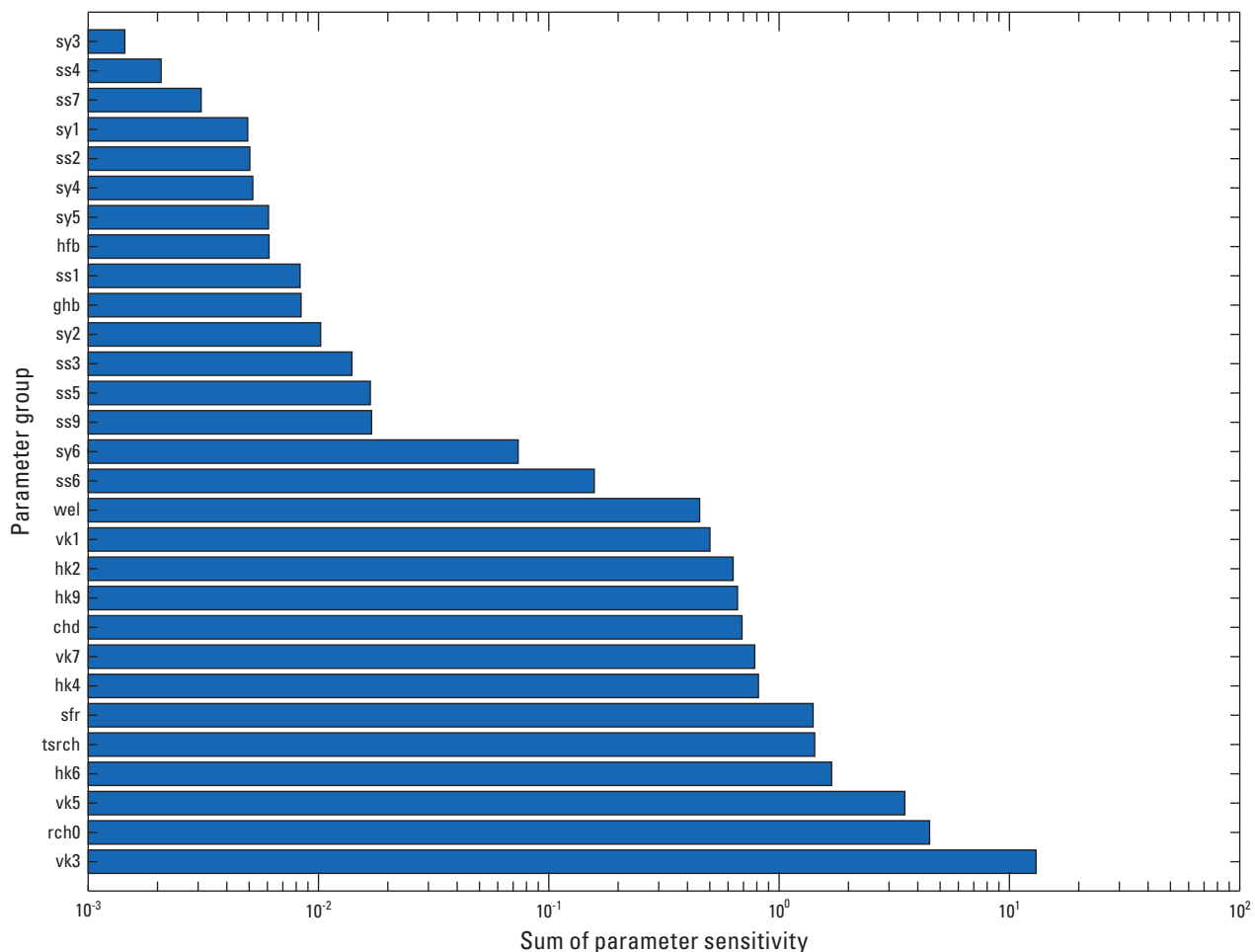


Figure 12. Parameter group sensitivities

valid because there is evidence of mixing of freshwater and saline groundwater (Hays and others, 2016). Therefore, the need for simulations including variable density may be warranted in local areas where high salinity water is problematic.

Lakes were not included in the Ozark system model. Although they locally affect the head in the aquifer and can be important sources or sinks for groundwater in the vicinity of the lake, the lake areas represent a relatively small part of the modeled surface area such that a given lake may cover only a few model cells. It is assumed that the contribution to the model water budget from lakes is minor relative to the overall model water budget. Quantifying interaction between lakes and groundwater in the Ozark system, which could be valuable based on the use of surface-water impoundments for water supply, would be better completed through focused efforts of higher-resolution data and possibly modeling localized areas.

The accuracy of water-use estimates and representation of pumping wells in the model is another important limitation to consider because of the role that pumping wells play in the simulated hydraulic-head and flow values. Water use was estimated by using a combination of 5-year county totals and site-specific pumping data extrapolated from about 1960 to 1900 (Knierim and others, 2017). Site-specific and

historical pumping data were sparse. Pumping was assumed to occur from the hydrogeologic unit intersecting the bottom of the well, such that pumping from wells open to multiple units was not explicitly modeled. Additionally, model cell size with respect to the location of pumping wells limits high-resolution characterization of groundwater levels. Because of the hydraulic properties in the Ozark system, such as low storage and localized zones of high hydraulic conductivity, water levels tend to vary by large amounts over short distances. Pumping wells are always modeled at cell centers, although observations of groundwater-level altitude are located at the true well location, such that the distance between a pumping well and observation data can be greater than 0.5 mi. In some cases, this distance can account for large discrepancies, even though the model may simulate acceptable drawdowns near the pumping well.

The hydrogeologic framework of an aquifer system establishes the driving force and boundaries constraining groundwater flow (Hays and others, 2016). The altitude and thickness of hydrogeologic units are the basis for the model framework and are based on available information, which varies spatially and vertically throughout the model area (Westerman and others, 2016a, b). Areas of sparse information may affect model results through assumptions in the altitude

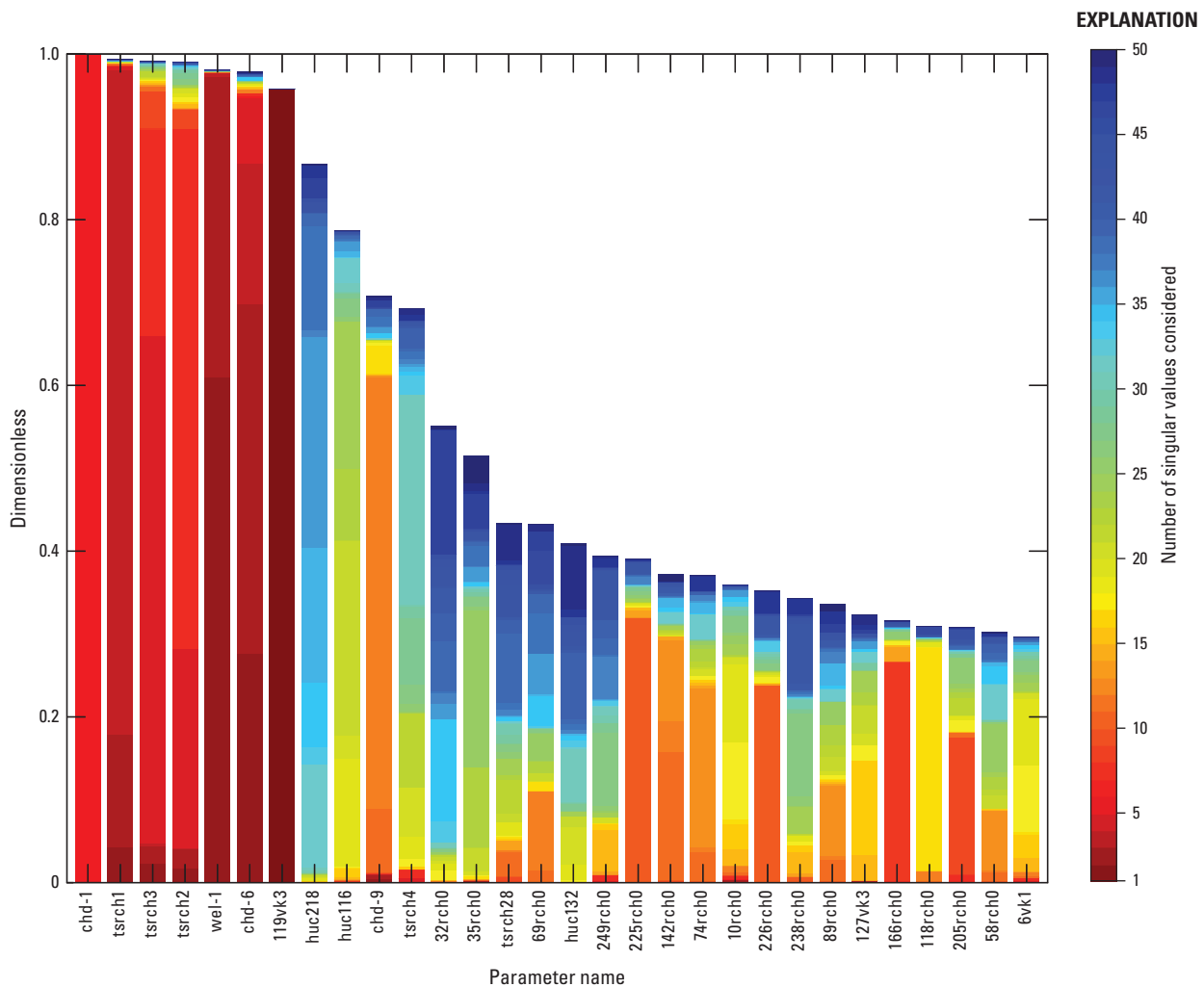


Figure 13. Parameter identifiability of the top 30 pilot-point parameters in the model. Parameter group names are defined in table 2.

and thickness of these hydrogeologic units and the lack of definition of structural controls that may affect groundwater movement. Additionally, small-scale lithologic changes (horizontally or vertically) that may be important for local groundwater flow (such as chert units within layer 1) are not modeled at the regional scale of the Ozark model.

Results of the Ozark model must also be evaluated in the context of temporal constraints. Streamflow and hydraulic-head data during predevelopment conditions are sparse to nonexistent; therefore, model calibration to predevelopment conditions are not well constrained. The temporal discretization of the model varies from 6 months to 40 years in stress-period length. Each stress period incorporates average input values for pumpage and precipitation for the given time interval; therefore, higher-resolution fluctuations (such as storm-event responses) are not represented in the model, although they can be critically important for groundwater flow at local scales.

One goal of the Ozark groundwater availability study was to develop a groundwater-flow model capable of suitable accuracy at regional scales, that is across a principal

aquifer system that covers 68,000 mi² horizontally and nine hydrogeologic units over several thousand feet vertically. The intent was not to reproduce individual local-scale details, which are typically not possible given the uniform cell size of 1 mi². Local-scale studies of groundwater flow are especially critical in karst systems where groundwater discharge can fluctuate rapidly in response to storm events and groundwater flow can cross surface-water divides. However, a regional-scale groundwater-flow model is not meant to—nor able to—capture flow at these higher temporal and spatial scales. For example, a large part of the water recharged to the Ozark system is discharged to springs and streams, such that—typical of karst systems—groundwater provides an important component of surface-water flow. Groundwater use from the Ozark system may be considered in the context of both consumptive use via groundwater pumping and instream use via groundwater maintenance of base flow. Therefore, the Ozark groundwater availability study coupled with surface-water modeling can aid water-resource managers trying to understand hydrologic flow requirements for supporting aquatic ecosystems. Scenarios of

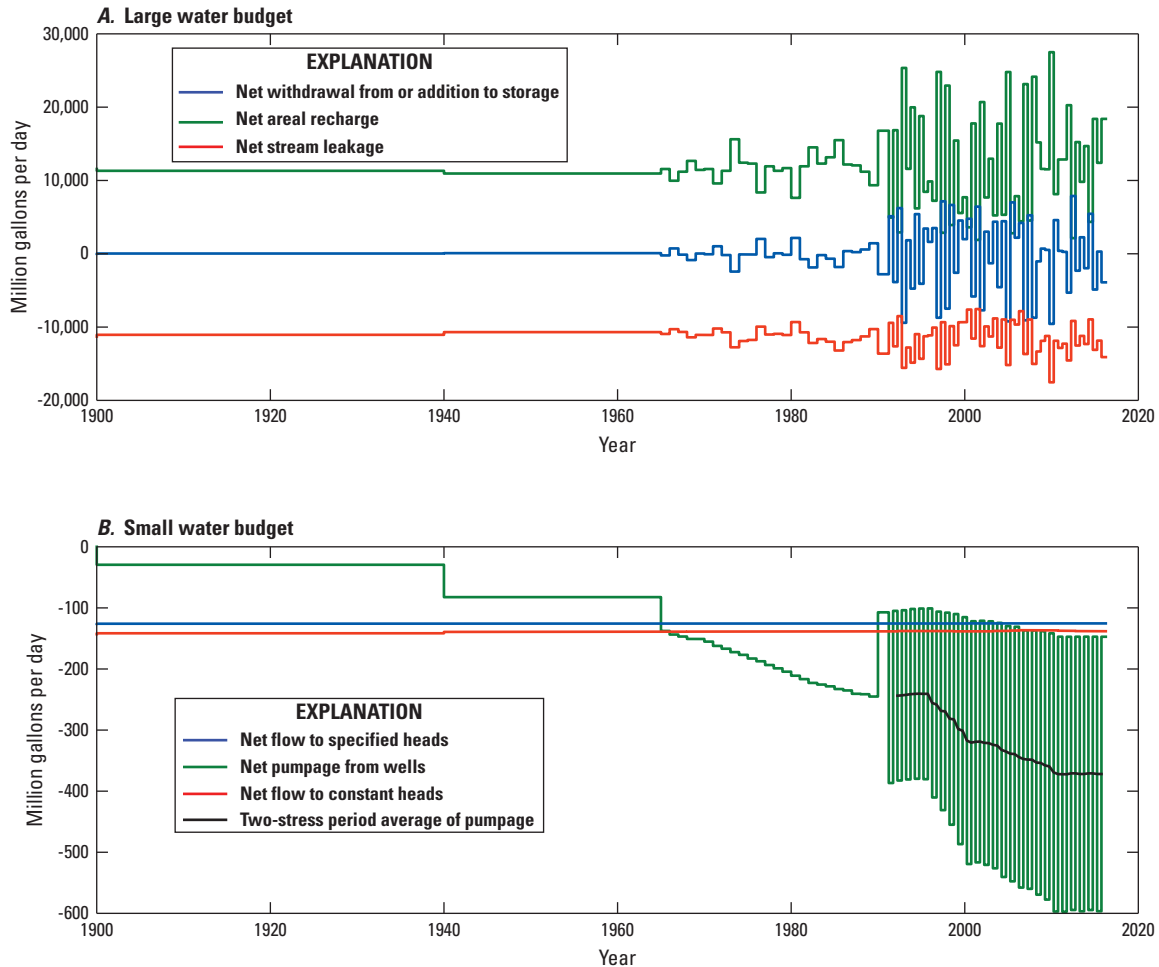


Figure 14. Groundwater-flow budget of *A*, large water-budget components and *B*, small water-budget components.

changing groundwater pumping and climate can be simulated by the Ozark model to quantify groundwater availability during periods of decreased recharge or increased pumping. Additionally, for future modeling efforts in the Ozark system either refined to a smaller model grid cell or covering a smaller spatial area, the current model may be used to determine the worth of potential observations that could reduce uncertainty predictions of groundwater-level altitudes or flow.

Summary

Groundwater in the Ozark Plateaus aquifer system (hereafter referred to as the Ozark system) is an important source for municipal, industrial, agricultural, and domestic water supply needs across much of southern Missouri, northern Arkansas, and smaller areas of southeastern Kansas and northeastern Oklahoma. A groundwater-flow model has been developed as the primary tool for the assessment of groundwater availability in the Ozark system.

The Ozark system study area, which corresponds to the Ozark model area, encompasses approximately 68,000 square miles (mi^2) over parts of four States, Arkansas, Kansas, Missouri, and Oklahoma, in the central United States. The model area was discretized horizontally into 1- mi^2 cells and vertically into 9 layers representing the Western Interior Plains confining unit, Springfield Plateau aquifer, Ozark confining unit, upper Ozark aquifer, middle Ozark aquifer, lower Ozark aquifer, St. Francois confining unit, upper St. Francois aquifer, and the lower St. Francois aquifer. The U.S. Geological Survey groundwater-flow model, MODFLOW-NWT, was used to approximate the solution of the equations governing three-dimensional groundwater flow.

The model simulates 116 years (1900–2015) of system response to stress by using 79 stress periods. Semiseasonal stress periods were simulated from the later part of 1991–2015 and represent higher demand and lower recharge in the spring and summer months and lower demand and higher recharge in the fall and winter months.

Hydrologic stresses and boundaries represented in the model include recharge, groundwater pumping, streams, specified heads, and faults. Estimates of recharge were determined with the Empirical-Water Balance method. Temporal changes in precipitation were used to adjust recharge in the model from 1900 to 1990 and semiseasonal recharge is used in the model from 1990 to 2015. Groundwater pumping for the model was estimated for the period 1900–2015 by using site-specific data from numerous sources in combination with countywide water-use estimates. Streams in the model were based on the National Hydrography Dataset and include those with a stream order greater than one. Boundaries representing flow along the perimeter of the model area include a head-dependent boundary in the southeastern part of the model area to represent the adjacent Mississippi embayment sediments and a constant head boundary along the western edge of the model. Some major faults are simulated in the model to limit lateral flow across the faulted region.

Hydraulic properties including horizontal and vertical hydraulic conductivity, specific yield, and specific storage were represented as parameters through pilot points or uniform values for an entire layer by using initial values from previous modeling efforts and interpretations from pumping data. Initial hydraulic conductivity in selected layers was allowed to vary spatially through the use of pilot points.

History matching for the Ozark model was accomplished by a combination of manual changes to parameter values and automated calibration methods. Automated parameter estimation was achieved through the use of parameter estimation software. Observation data used included 19,045 hydraulic-head observations from 6,683 wells within the Ozark model area. Observation data also included stream leakage estimates summed to calculate a net gain or loss value for each stream.

Parameter identifiability indicates how well a parameter may be constrained by the observations used in history matching. Identifiability of the top 30 pilot points differ somewhat from the most sensitive parameters, indicating that parameter correlation may have an effect on some parameters. The majority of the recharge component is discharged through streams, fluctuating seasonally between 7,500 and 17,500 million gallons per day (Mgal/d) with a mean outflow of 11,500 Mgal/d. Much of the remaining balance between recharge inflows and stream outflows is made up by water moving into or out of storage in the system. Groundwater pumping increases throughout the simulation period, with a maximum rate of about 600 Mgal/d.

An understanding of model limitations is essential to effectively use flow and hydraulic-head simulation results. The goal of the Ozark model was to develop a model capable of suitable accuracy at regional scales. The intent was not to reproduce individual local-scale details, which are typically not possible given the uniform cell size of 1 mi². Although the Ozark model may not represent each local-scale detail, it is relevant for a better understanding of the regional flow system.

References Cited

- Adamski, J.C., Petersen, J.C., Freiwald, D.A., and Davis, J.V., 1995, Environmental and hydrologic setting of the Ozark Plateaus study unit, Arkansas, Kansas, Missouri, and Oklahoma: U.S. Geological Survey Water-Resources Investigations Report 94–4022, 76 p.
- Brye, K.R., West C.P., and Gbur, E.E., 2004, Soil quality differences under native tallgrass prairie across a climosequence in Arkansas: *The American Midland Naturalist*, v. 152, no. 2, p. 214–230.
- Clark, B.R., Westerman, D.A., and Fugitt, D.T., 2013, Enhancements to the Mississippi Embayment Regional Aquifer Study (MERAS) groundwater-flow model and simulations of sustainable water-level scenarios: U.S. Geological Survey Scientific Investigations Report 2013–5061, 29 p., accessed December 29, 2017, at <http://pubs.usgs.gov/sir/2013/5161/>.
- Czarnecki, J.B., Gillip, J.A., Jones, P.M., and Yeatts, D.S., 2009, Groundwater-flow model of the Ozark Plateaus aquifer system, northwestern Arkansas, southeastern Kansas, southwestern Missouri, and northeastern Oklahoma: U.S. Geological Survey Scientific Investigations Report 2009–5148, 62 p. (Revised March 2010.)
- Doherty, John, 2003, Groundwater model calibration using pilot-points and regularization: *Ground Water*, v. 41, no. 2, p. 170–177, accessed March 20, 2018, at <https://doi.org/10.1111/j.1745-6584.2003.tb02580.x>.
- Doherty, John, 2010, PEST, Model-independent parameter estimation—User manual (5th ed., with slight additions): Brisbane, Australia, Watermark Numerical Computing, [333 p.] accessed November 13, 2014, at <http://www.pesthomepage.org/Downloads.php>.
- Doherty, John, 2011, Groundwater data utilities, part A: Overview: Watermark Numerical Computing, February 2011, accessed January 21, 2012, at <http://www.pesthomepage.org/Downloads.php>.
- Doherty, John, and Hunt, R.J., 2009, Two statistics for evaluating parameter identifiability and error reduction: *Journal of Hydrology*, v. 366, no. 1–4, p. 119–127, accessed December 29, 2017, at <http://dx.doi.org/10.1016/j.jhydrol.2008.12.018>.
- Duncan, L.L., and Clark, B.R., 2018, MODFLOW-NWT model of groundwater flow in the Ozark Plateaus aquifer system: U.S. Geological Survey data release, <https://doi.org/10.5066/F718350W>.
- Fienen, M.N., Muffels, C.T., and Hunt, R.J., 2009, On constraining pilot point calibration with regularization in PEST: *Ground Water*, v. 47, no. 6, p. 835–844, accessed December 29, 2017, at <http://dx.doi.org/10.1111/j.1745-6584.2009.00579.x>.

- Feinstein, D.T., Hunt, R.J., and Reeves, H.W., 2010, Regional groundwater-flow model of the Lake Michigan Basin in support of Great Lakes Basin water availability and use studies: U.S. Geological Survey Scientific Investigations Report 2010–5109, 379 p.
- Harbaugh, A.W., 2005, MODFLOW–2005, The U.S. Geological Survey modular ground-water model—The ground-water flow process: U.S. Geological Survey Techniques and Methods book 6, chap. A16, variously paged.
- Harbaugh, A.W., and Hill, M.C., 2009, Observations in MODFLOW–2005—File OBS.pdf distributed with MODFLOW–2005: U.S. Geological Survey, 32 p. (Also available at <https://water.usgs.gov/ogw/modflow/index.html>.)
- Hays, P.D., Knierim, K.J., Breaker, B.K., Westerman, D.A., and Clark, B.R., 2016, Hydrogeology and hydrologic conditions of the Ozark Plateaus aquifer system: U.S. Geological Survey Scientific Investigations Report 2016–5137, 61 p., accessed December 29, 2017, at <http://dx.doi.org/10.3133/sir20165137>.
- Hill, M.C., and Østerby, Ole, 2003, Determining extreme parameter correlation in ground water models: Ground Water, v. 41, no. 4, p. 420–430 accessed March 20, 2018, at <https://doi.org/10.1111/j.1745-6584.2003.tb02376.x>.
- Hunt, R.J., Doherty, John, and Tonkin, M.J., 2007, Are models too simple? Arguments for increased parameterization: Ground Water, v. 45, no. 3, p. 254–262.
- Imes, J.L., 1989, Analysis of the effect of pumping on ground-water flow in the Springfield Plateau and Ozark aquifers near Springfield, Missouri: U.S. Geological Survey Water Resources Investigations Report 89–4079, 63 p.
- Imes, J.L., and Emmett, L.F., 1994, Geohydrology of the Ozark Plateaus Aquifer System in parts of Missouri, Arkansas, Oklahoma, and Kansas: U.S. Geological Survey Professional Paper 1414–D, 140 p.
- Jorgensen, D.G., Helgesen, J.O., and Imes, J.L., 1993, Regional aquifers in Kansas, Nebraska, and parts of Arkansas, Colorado, Missouri, New Mexico, Oklahoma, South Dakota, Texas, and Wyoming: geohydrologic framework: U.S. Geological Survey Professional Paper 1414–B, accessed September 9, 2015, at <http://pubs.er.usgs.gov/publication/pp1414B>.
- Knierim, K.J., Wagner, D.M., Roland, V.L., and Nottmeier, A.M., 2015, Ozark Plateaus seepage run dataset, southern Missouri and northern Arkansas, 1982–2006: U.S. Geological Survey data release, <http://dx.doi.org/10.5066/F7W9577Q>.
- Knierim, K.J., Nottmeier, A.M., Worland, S., Westerman, D.A., and Clark, B.R., 2016, Groundwater withdrawal rates from the Ozark Plateaus aquifer system, 1900 to 2010, U.S. Geological Survey data release, <https://dx.doi.org/10.5066/F7GQ6VV1>.
- Knierim, K.J., Nottmeier, A.M., Worland, S., Westerman, D.A., and Clark, B.R., 2017, Challenges for creating a site-specific groundwater use record for the Ozark Plateaus aquifer system from 1900 to 2010: Hydrogeology Journal, v. 25, no. 6, p. 1779–1793, accessed March 20, 2018, at <https://doi.org/10.1007/s10040-017-1593-1>.
- Macfarlane, P.A., and Hathaway, L.R., 1987, The hydrogeology and chemical quality of ground waters from the lower Paleozoic aquifers in the Tri-State region of Kansas, Missouri, and Oklahoma: Kansas Geological Survey Ground-Water Series 9, 37 p.
- McKay, L., Bondelid, T., Dewald, T., Johnston, J., Moore, R., and Rea, A., 2012, NHDPlus Version 2: User Guide: U.S. Environmental Protection Agency, 172 p.
- Missouri Department of Natural Resources, 2017, Groundwater-level observation well network: Missouri Department of Natural Resources, accessed June 16, 2017 at <https://dnr.mo.gov/geology/wrc/groundwater/gwnetwork.htm?env/wrc/groundwater/gwnetwork.htm>.
- Nelson, P.H., Gianoutsos, N.J., and Drake, R.M., 2015, Under pressure in Mesozoic and Paleozoic rock units in the Midcontinent of the United States: Association of Petroleum Geologists Bulletin, v. 99, no. 10, p. 1861–1892, accessed December 29, 2017, at <https://doi.org/10.1306/04171514169>.
- Niswonger, R.G., Panday, Sorab, and Ibaraki, Motomu, 2011, MODFLOW–NWT, A Newton formulation for MODFLOW–2005: U.S. Geological Survey Techniques and Methods book 6, chap. A37, 44 p.
- Niswonger, R.G., and Prudic, D.E., 2005, Documentation of the Streamflow-Routing (SFR2) Package to include unsaturated flow beneath streams—A modification to SFR1: U.S. Geological Survey Techniques and Methods book 6, chap. A13, 48 p.

- Nottmeier, A.M., 2015, Regional potentiometric surface of the Ozark aquifer in Arkansas, Kansas, Missouri, and Oklahoma, November 2014–January 2015: U.S. Geological Survey Scientific Investigations Map 3348, 1 sheet, accessed December 29, 2017, at <http://dx.doi.org/10.3133/sim3348>.
- Reitz, M.D., Sanford, W.E., Senay, G.B., and Cazenaz, Jeffrey, 2015, Annual regression-based estimates of evapotranspiration for the contiguous United States based on climate, remote sensing, and stream gage data: American Geophysical Union, proceedings, accessed January 30, 2017, at <https://agu.confex.com/agu/fm15/webprogram/Paper84061.html>.
- Reitz, M.D., Sanford, W.E., Senay, G.B., and Cazenaz, Jeffrey, 2017, Annual estimates of recharge, quick-flow runoff, and evapotranspiration for the contiguous U.S. using empirical regression equations: *Journal of the American Water Resources Association*, v. 53, no. 4, 23 p., access December 29, 2017, at <https://doi.org/10.1111/1752-1688.12546>.
- Richards, Joseph M., 2010, Groundwater-flow model and effects of projected groundwater use in the Ozark Plateaus Aquifer System in the vicinity of Greene County, Missouri – 1907-2030: U.S. Geological Survey Scientific Investigations Report 2010-5227, 106 p.
- Stoeser, D.B., Green, G.N., Morath, L.C., Heran, W.D., Wilson, A.B., Moore, D.W., and Van Gosen, B.S., 2005, Preliminary integrated geologic map databases for the United States: Central States: Montana, Wyoming, Colorado, New Mexico, Kansas, Oklahoma, Texas, Missouri, Arkansas, and Louisiana: U.S. Geological Survey Open-File Report 2005-1351, accessed December 29, 2017, at <https://pubs.er.usgs.gov/publication/ofr20051351>.
- Tikhonov, A.N., 1963, Regularization of incorrectly posed problems: *Soviet Mathematics Doklady*, v. 4, p. 1624–1637.
- Tonkin, M.J., and Doherty, John, 2005, A hybrid regularized inversion methodology for highly parameterized environmental models: *Water Resources Research*, v. 41, no. 10, accessed December 29, 2017, at <http://dx.doi.org/10.1029/2005WR003995>.
- U.S. Geological Survey, 2016, USGS water availability and use science program, accessed December 2, 2016, at <https://water.usgs.gov/wausp/>.
- U.S. Geological Survey, 2017a, The national map, accessed November 13, 2017, at <https://nationalmap.gov>.
- U.S. Geological Survey, 2017b, Hydrologic unit maps, accessed February 22, 2017, at <https://water.usgs.gov/GIS/huc.html>.
- Welter, D.E., White, J.T., Hunt, R.J., and Doherty, J.E., 2015, Approaches in highly parameterized inversion—PEST++ Version 3, a Parameter ESTimation and uncertainty analysis software suite optimized for large environmental models: U.S. Geological Survey Techniques and Methods, book 7, chap. C12, 54 p., accessed December 29, 2017, at <http://dx.doi.org/10.3133/tm7C12>.
- Westenbroek, S.M., Kelson, V.A., Dripps, W.R., Hunt, R.J., and Bradbury, K.R., 2010, SWB—A modified Thornthwaite-Mather Soil-Water-Balance code for estimating groundwater recharge: U.S. Geological Survey Techniques and Methods book 6, chap. A31, 60 p.
- Westerman, D.W., Gillip, J.A., Richards, J.M., Hays, P.D., and Clark, B.R., 2016a, Altitudes and thicknesses of hydrogeologic units of the Ozark Plateaus aquifer system in Arkansas, Kansas, Missouri, and Oklahoma: U.S. Geological Survey data release, accessed December 29, 2017, at <http://dx.doi.org/10.5066/F7HQ3X0T>.
- Westerman, D.W., Gillip, J.A., and Richards, J., Hays, P.D., and Clark, B.R., 2016b, Altitudes and thicknesses of hydrogeologic units of the Ozark Plateaus aquifer system in Arkansas, Kansas, Missouri, and Oklahoma: U.S. Geological Survey Scientific Investigations Report, 2016-5130, 32 p., accessed December 29, 2017, at <https://pubs.er.usgs.gov/publication/sir20165130>.
- Wittman, J.W., Kelson, V., and Wilson, T., 2003, Final report: Source of supply investigation for Joplin, Missouri: Wittman Hydro Planning Associates, Inc., 97 p.

Prepared by the Lafayette Publishing Service Center

For more information about this publication, contact
Director, Lower Mississippi-Gulf Science Center
U.S. Geological Survey
401 Hardin Road
Little Rock, AR 72211
(501) 228-3600

For additional information visit
<https://www.usgs.gov/centers/lmg-water/>

